STEM CELLS®

Original Article

Roles of Stat3 and ERK in G-CSF Signaling

KENJIROU KAMEZAKI,[a,b] KAZUYA SHIMODA,[a,b] AKIHIKO NUMATA,[a,b] TAKASHI HARO,[a,b] HARUKO KAKUMITSU,[a,b] MASUMI YOSHIE,[c] MASAHIRO YAMAMOTO,[c] KIYOSHI TAKEDA,[d] TADASHI MATSUDA,[e] SHIZUO AKIRA,[d] KATSUHIRO OGAWA,[c] MINE HARADA[a,b]

[a]The First Department of Internal Medicine, Faculty of Medicine, Kyushu University, Fukuoka, Japan; [b]Medicine and Biosystemic Science, Kyushu University Graduate School of Medical Sciences, Fukuoka, Japan; [c]Department of Pathology, Asahikawa Medical College, Asahikawa, Japan; [d]Department of Host Defense, Research Institute for Microbial Diseases, Osaka University, Osaka, Japan; [e]Department of Immunology, Graduate School of Pharmaceutical Sciences, Hokkaido University, Sapporo, Japan

Key Words. Signal transduction • Hematopoiesis • Signal transducer and activator of transcription Mitogen-activated protein kinase • G-CSF

ABSTRACT

G-CSF specifically stimulates the proliferation and differentiation of cells that are committed to the neutrophil-granulocyte lineage. Although Stat3 was thought to be essential for the transduction of G-CSF–induced cell proliferation and differentiation signals, mice deficient for Stat3 in hematopoietic cells show neutrocytosis and infiltration of cells into the digestive tract. The number of progenitor cells in the neutrophil lineage is not changed, and G-CSF–induced proliferation of progenitor cells and prolonged neutrophil survival were observed in Stat3-deficient mice. In hematopoietic cells from Stat3-deficient mice, trace levels of SOCS3, a negative regulator of granulopoiesis, were observed, and SOCS3 expression was not induced by G-CSF stimulation. Stat3-null bone marrow cells displayed a significant activation of extracellular regulated kinase 1 (ERK1)/ERK2 under basal conditions, and the activation of ERK was enhanced and sustained by G-CSF stimulation. Furthermore, the augmented proliferation of Stat3-deficient bone marrow cells in response to G-CSF was dramatically decreased by addition of a MEK1 inhibitor. These results indicate that Stat3 functions as a negative regulator of G-CSF signaling by inducing SOCS3 expression and that ERK activation is the major factor responsible for inducing the proliferation of hematopoietic cells in response to G-CSF. STEM CELLS *2005;23:252–263*

INTRODUCTION

The proliferation and differentiation of hematopoietic precursor cells are regulated by a family of cytokines. In particular, granulocyte colony-stimulating factor (G-CSF) specifically stimulates the proliferation and differentiation of cells that are committed to the neutrophil lineage [1]. The biological functions of G-CSF are mediated through binding to a cell-surface receptor that is predominantly expressed on neutrophilic progenitor cells and mature neutrophilic granulocytes, although the receptor is also expressed on hematopoietic progenitor cells [2]. The binding of G-CSF to its receptor induces the tyrosine phosphorylation of Jak1, Jak2, and Tyk2 [3–6], which are members of the Janus family of protein tyrosine kinases (Jaks) [7]. Activated Jaks phosphorylate residues in the cytosolic

Correspondence: Kazuya Shimoda, M.D., The First Department of Internal Medicine, Faculty of Medicine, Kyushu University, 3-1-1 Maidashi, Higashi-ku, Fukuoka, Fukuoka 812-8582, Japan. Telephone: 81-92-642-5230; Fax: 81-92-642-5247; e-mail: kshimoda@intmed1.med.kyushu-u.ac.jp Received August 3, 2004; accepted for publication October 6, 2004. ©AlphaMed Press 1066-5099/2005/$12.00/0 doi: 10.1634/stemcells.2004-0173a

tails of G-CSF receptors, allowing subsequent recruitment of various signaling proteins to the receptor complex. Members of the signal transducers and activators of transcription (Stat) family are recruited and phosphorylated by Jak kinase, translocate to the nucleus, and bind the promoter regions of target genes [8, 9]. G-CSF stimulation results in the specific phosphorylation of Stat3 [4, 10] and, more infrequently, Stat5 and Stat1 [6, 11]. Generally, this Jak-Stat signaling pathway is thought to be essential for the transduction of cytokine signaling [12], but other cytoplasmic protein tyrosine kinases, including lyn and syk [13, 14], are also phosphorylated and activated in response to G-CSF signaling.

The role of Jak kinases in the G-CSF signaling pathway was initially examined by the use of cell lines that were deficient for each of the Jak kinases. G-CSF induces the tyrosine phosphorylation and activation of Jak1, Jak2, and Tyk2, and the absence of one Jak does not preclude G-CSF–induced tyrosine phosphorylation of the remaining Jaks. However, in the absence of Jak1, G-CSF does not induce receptor tyrosine phosphorylation, and the induced tyrosine phosphorylation of Stat proteins is greatly reduced [6]. Although multiple Jaks are activated by G-CSF, Jak1 is in a unique position to phosphorylate the receptor and thereby affect Stat protein tyrosine phosphorylation because of either location within the receptor complex or substrate specificity. However, Jak1-deficient mice do not show neutropenia, and Jak1 deficiency has no effect on the colony formation of bone marrow cells induced by G-CSF [15]. Furthermore, deletion of either Jak2 or Tyk2 has no effect on G-CSF–induced colony formation of bone marrow cells [16, 17]. These results indicate that there is redundancy among the Jak kinases in G-CSF signaling, and the lack of one Jak kinase may be compensated for by the activation of other Jak kinases. Interestingly, the involvement of Jak kinases in G-CSF signaling seems to be different from that in other cytokine-signaling pathways. For example, Jak1 is essential for gp130, interferon (IFN), and interleukin (IL-7)–mediated signaling [15]. Jak2 is essential for erythropoietin (Epo) signaling [17], Jak3 is essential for IL-2 receptor common gamma chain–mediated signaling [15], and Tyk2 is essential for IL-12 signaling [16].

In addition, we and others have used Stat-deficient mice to demonstrate that Stats play an essential and nonredundant role in cytokine signaling [18–22]. G-CSF stimulation activates mainly Stat3 and, to a lesser extent, Stat1 and Stat5 in bone marrow cells. Stat1 and Stat5a/b-deficient mice have normal neutrophil numbers, although colony formation by bone marrow cells in response to G-CSF stimulation is decreased by the absence of Stat5a/b [18, 21]. However, the expression of dominant-negative Stat3 in 32Dcl3 cells, which differentiate into neutrophils after G-CSF treatment, does not prevent them from proliferating in response to G-CSF [23]. Additionally, transgenic mice with a targeted mutation of the G-CSF receptor that abolishes G-CSF–dependent Stat3 activation show severe neutropenia, with an accumulation of immature myeloid precursors in the bone marrow [24]; constitutively active Stat3 partially rescues this neutropenia. Stat3 is then thought to transduce the proliferation and differentiation signal of G-CSF. Ablation of Stat3 produced early embryonic lethality [25], and selective ablation of Stat3 in neutrophils and monocytes by Cre recombinase-dependent gene deletion directed by the macrophage lysozyme promoter did not affect neutrophil production, suggesting that Stat3 is required at an early stage of neutrophil development. To clarify the role of Stat3 in the G-CSF signaling pathway, we have examined the role of Stat3 in hematopoiesis by selective ablation of the *Stat3* gene in hematopoietic progenitor cells. In contrast to expectations, mice that were deficient for *Stat3* in hematopoietic cells show neutrocytosis and infiltration of cells into the digestive tract.

Materials and Methods

Mice

$Stat3^{flox/-}$ mice were generated by mating $Stat3^{flox/+}$ mice, in which the DNA base pairs encoding the tyrosine phosphorylation site in Stat3 are flanked by two loxP sites ($Stat3^{flox/flox}$) [26], with $Stat3^{+/-}$ mice, in which exons 20 through 22 are replaced by a neomycin resistance gene in the knockout allele [27]. To establish mice with a conditional knockout of Stat3 in hematopoietic cells, $Stat3^{flox/-}$ mice were mated with a transgenic line bearing Cre recombinase driven by the IFN-inducible Mx promoter [28]. Genotyping was performed by polymerase chain reaction analysis of genomic tail DNA. The primer sequences were as follows: Stat3-flox: 5'-cctgaagaccaagttcatctgtgtgac-3' and 5'-cacacaagccatcaaactctggtctcc-3'; $Stat3^{-}$: 5'-agcagctgacaacgctggctgagaagct-3' and 5'-atcgccttctatcgccttcttgacgag-3'; Mx1-Cre: 5'-ggacatgttcagggatcgccaggcg-3' and 5'-gcataaccagtgaaacagcattgctg-3'. Expression of Cre was induced by injecting mice intraperitoneally with 250 μg of polyinocinic-polycytidylic acid (pIpC) (Sigma, St. Louis) three times at 2-day intervals as previously described [28]. Age-matched $Stat3^{flox/-}$ and Mx1-Cre:$Stat3^{flox/-}$ were injected with pIpC and used for further experiments 2 weeks later, except where noted in the text. Mice were housed and bred in the Kyushu University Animal Center.

Histological and Hematological Analysis

Tissues were fixed in 10% phosphate-buffered formalin, and paraffin-embedded tissue sections were stained with hematoxylin and eosin using standard techniques.

Complete blood counts were analyzed using Celltac α (Nihon Kohden, Tokyo). Peripheral and bone marrow blood

cells were prepared on slide glasses and stained with Giemsa solution. Differential cell counts were scored visually.

Preparation of Neutrophils from the Peritoneal Cavity

Mice were injected intraperitoneally with 2 ml of 4% thioglycollate. After 4 hours, peritoneal neutrophils were obtained by peritoneal lavage with 10 ml of ice-cold phosphate-buffered saline (PBS). After an 8-hour incubation in plastic dishes, nonadherent cells were harvested and used for further experiments. These cells were >90% Gr-1$^+$, as determined by flow cytometry.

Evaluation of Apoptosis

To evaluate apoptosis, cells were incubated with fluorescein isothiocyanate (FITC)–conjugated Gr1 (Becton, Dickinson, San Jose, CA) and propidium iodide for 30 minutes at 4°C, washed twice in PBS, and analyzed on a FACS Calibur (Becton, Dickinson). To exclude the dead cells, the gated nucleated cells were used for further examination.

Chemotaxis Assay

The neutrophil chemotaxis assay was performed as described [29]. Briefly, the lower well contained 800 μl of Iscove's modified Dulbecco's medium (IMDM) supplemented with 10% fetal calf serum (FCS) and 1×10^{-7} M formyl-methionyl-leucyl-phenylalanine (fMLP) (Sigma), and the upper chemotaxicell (Kurabo, Osaka) chamber contained 400 μl of a neutrophil suspension. After incubation for 1 hour at 37°C, the cells that had passed through the membrane were counted.

Hematopoietic Progenitor Cell Assays

The frequency of hematopoietic progenitor cells was determined by clonogenic assays in methylcellulose, as described previously [30]. Briefly, bone marrow or peripheral blood mononuclear cells were separated by Ficoll-Paque sedimentation, and 1×10^5 or 2×10^5 cells were cultured in methylcellulose containing IL-3 (20 ng/ml), stem cell factor (SCF) (20 ng/ml), and Epo (4 U/ml) for the colony-forming unit-granulocyte, macrophage (CFU-GM), BFU-E, and CFU-culture (CFU-C) assays or G-CSF (50 ng/ml) only for the CFU-G assay. CFU-GM, CFU-G, and BFU-E were measured after 10 days in culture.

In Vitro Proliferation Assays

Bone marrow mononuclear cells (1×10^6/ml) were incubated for 3 days in IMDM supplemented with 30% FCS in the presence or absence of IL-3 (1 ng/ml) and G-CSF (10 ng/ml). To assess the effects of an MEK inhibitor, dimethyl sulfoxide (DMSO) or U0126 (Cell Signaling, Beverly, MA) dissolved in DMSO was added. After 72 hours, 0.5 μCi ^{3}H-thymidine was added and the cells were incubated for an additional 8 hours. Proliferative activity was determined by ^{3}H-thymidine incorporation.

In Vivo Administration of G-CSF or Thrombopoietin

Mice were injected subcutaneously with either G-CSF (50 μg/kg daily for the indicated period) or with thrombopoietin (TPO) (30 μg/kg for 5 days). Peripheral blood was collected on the indicated day.

Dextran Sulfate Sodium–Induced Colitis (DSS)

Colitis was induced by feeding mice drinking water supplemented with 4% DSS (Wako, Osaka, Japan), as described previously [31]. Control mice were fed drinking water without DSS.

Western Blotting

Bone marrow cells were treated with G-CSF for the indicated time and were then lysed in lysis buffer as previously described [32]. Cell lysates were centrifuged at 12,000*g* for 15 minutes to remove debris. Total cell lysates were resolved by sodium dodecyl sulfate-10% polyacrylamide gel electrophoresis and transferred to a nitrocellulose membrane. Membranes were probed using the indicated antibodies and visualized with an ECL detection system (Amersham, Uppsala, Sweden). Anti-phospho-ERK1/2, anti-phospho-p38, anti-ERK2, anti-phospho-Stat3, and anti-phospho-Stat5 antibodies were purchased from Cell Signaling. Anti-Stat3 and anti-Stat5 antibodies were purchased from Santa Cruz Biotechnology (Santa Cruz, CA). Anti-SOCS3 antibody was purchased from IBL (Gunma, Japan).

Results

Increased Numbers of Circulating Neutrophils and Myeloid Cells in the Bone Marrow in Stat3-Deficient Mice

To determine whether Stat3 plays a role in hematopoiesis, we used the Cre-loxP recombination system. To decrease the amount of residual Stat3 protein after Cre-mediated deletion, we crossed Stat3$^{flox/-}$ mice with a transgenic line bearing Cre recombinase driven by the IFN-inducible Mx promoter. Only trace amounts of Stat3 were detected after induction of Mx-Cre by treatment with pIpC (Fig. 1A). When bone marrow cells from pIpC-treated Mx1:Stat3$^{flox/-}$ mice were treated with G-CSF, the phosphorylation of Stat3 was diminished, whereas Stat5 was phosphorylated at the same extent as wild-type mice by IL-3 stimulation.

We next examined the role of Stat3 in granulopoiesis in vivo. Blood cell counts from wild-type and Mx1:Stat3$^{flox/-}$

Table 1. Complete blood counts

	$Stat3^{flox/-}$	$Mx1:Stat3^{flox/-}$
White blood cell (× $10^3/\mu L$)	6.64 ± 2.23	7.84 ± 2.57
Neutrophil (per μL)	1,800 ± 953	4,172 ± 1,889
Lymphocyte (per μL)	3,868 ± 1,552	2,787 ± 1,009
Monocyte (per μL)	664 ± 359	522 ± 295
Eosinophil (per μL)	256 ± 225	324 ± 267
Hematocrit (%)	47.4 ± 2.2	45.7 ± 2.6
Platelet (× $10^4/\mu L$)	80.7 ± 27.6	75.1 ± 22.4

Peripheral blood count analyses from polyinocinic-polycytidylic acid–treated $Stat3^{flox/-}$ and $Mx1:Stat3^{flox/-}$ mice (n = 18) at ages of 7–10 weeks. White blood cell differential counts were examined by Giemsa staining.

littermates 2 weeks after deletion of Stat3 are shown in Table 1. Morphologically identifiable neutrophils were detected in the peripheral blood of mice lacking Stat3 in hematopoietic cells, and the number of circulating neutrophils in $Mx1:Stat3^{flox/-}$ mice was 2.3-fold greater than in control mice. There were no differences in the numbers of lymphocytes, erythrocytes, or platelets due to ablation of Stat3. In bone marrow, the number of mature myeloid cells was greater in $Mx1:Stat3^{flox/-}$ mice than in control littermates, which is consistent with the observations in peripheral blood (Fig. 1B).

Effects of Stat3 Deletion on the Frequency of Myeloid and Erythroid Progenitor Cells and on the Response to G-CSF in Bone Marrow Cells

Because the number of neutrophils was higher in the $Mx1:Stat3^{flox/-}$ mice, we next determined the number of hematopoietic progenitor cells in the bone marrow. Bone marrow from pIpC-treated control or $Mx1:Stat3^{flox/-}$ mice was seeded in methylcellulose containing IL-3, SCF, and Epo to determine CFU-GM or in methylcellulose containing G-CSF to determine CFU-G. The CFU-GM and BFU-E cloning efficiencies were comparable in $Stat3^{flox/-}$ and $Mx1:Stat3^{flox/-}$ bone marrow cells in the presence of IL-3, SCF, and Epo (Fig. 2A). Similarly, the total colony numbers were not altered due to the absence of Stat3 (data not shown). The number of CFU-G induced by G-CSF was also unaffected by the absence of Stat3 (Fig. 2A).

Because the number of myeloid progenitor cells was not affected by the absence of Stat3, we next examined the effect of Stat3 deletion in bone marrow cells for the proliferation by cytokine stimulation. Bone marrow cells taken from $Mx1:Stat3^{flox/-}$ mice and $Stat3^{flox/-}$ mice 14 days after pIpC treatment responded to IL-3 to a similar extent. In contrast, the proliferation of bone marrow cells after G-CSF stimulation was enhanced in $Mx1:Stat3^{flox/-}$ mice 14 days after pIpC treatment compared with control littermates (Fig. 2B).

To examine the possibility that Stat3 is involved in G-CSF–mediated cell survival, we determined the susceptibility of neutrophils to apoptosis in the presence of 10 ng/ml of G-CSF (Fig. 2C). After 48 hours in media supplemented with G-CSF, there was

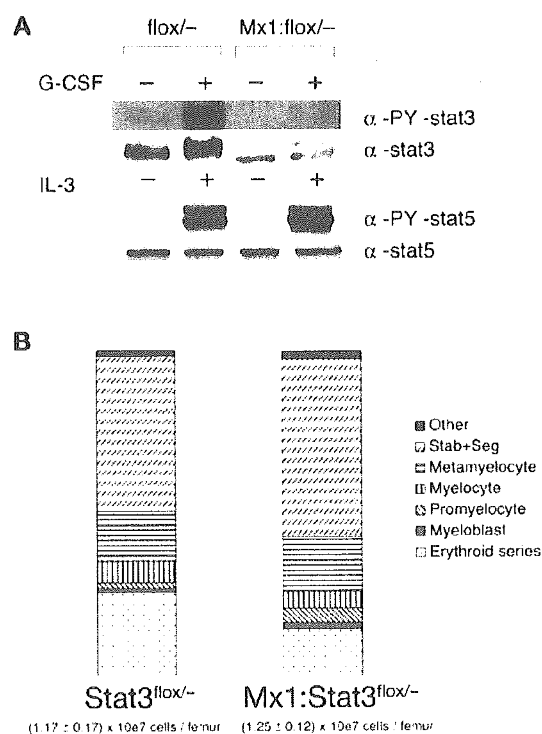

Figure 1. (A): Phosphorylation of Stat3 or Stat5 in response to G-CSF or IL-3 stimulation of bone marrow cells from $Stat3^{flox/-}$ and $Mx1:Stat3^{flox/-}$ mice. Bone marrow cells from $Stat3^{flox/-}$ and $Mx1:Stat3^{flox/-}$ mice were incubated for 8 hours in the absence of cytokines and then stimulated with G-CSF (50 ng/ml) or IL-3 (10 ng/ml) for 30 minutes. Total cell lysates were analyzed by Western blot with the indicated antibodies. **(B):** Bone marrow analysis from $Stat3^{flox/-}$ and $Mx1:Stat3^{flox/-}$ mice. Bone marrow differential counts were performed on preparations from $Stat3^{flox/-}$ and $Mx1:Stat3^{flox/-}$ mice that were euthanized 2 weeks after treatment with polyinocinic-polycytidylic acid. Abbreviation: IL, interleukin.

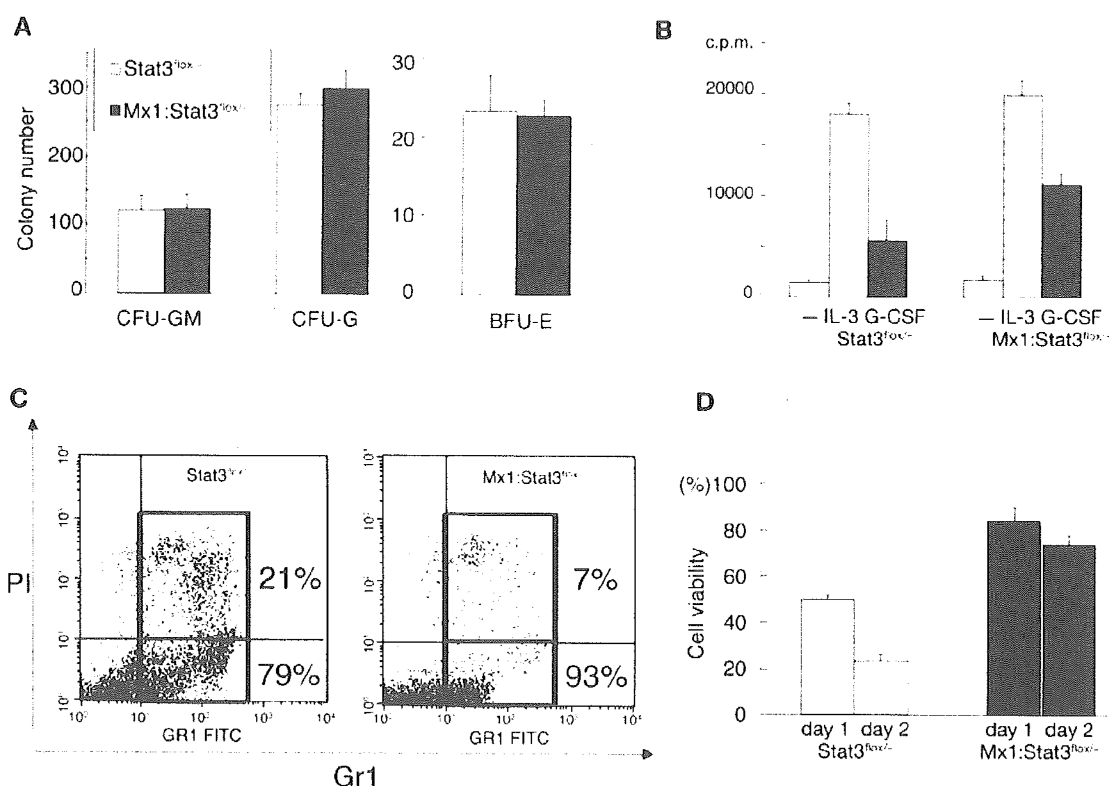

Figure 2. (A): In vitro colony formation by bone marrow cells from Stat3$^{flox/-}$ and Mx1:Stat3$^{flox/-}$ mice. Bone marrow cells (1×10^5/plate) from Stat3$^{flox/-}$ or Mx1:Stat3$^{flox/-}$ mice were plated in methylcellulose containing IL-3 (20 ng/ml), stem cell factor (20 ng/ml), and erythropoietin (4 U/ml) for the CFU-GM and BFU-E assays or G-CSF (50 ng/ml) only for the CFU-G assay. CFU-GM, BFU-E, and CFU-G were measured after 10 days in culture. **(B):** Proliferative activity of bone marrow cells in response to IL-3 and G-CSF. Bone marrow cells (1×10^6/ml) were incubated for 3 days in the presence of IL-3 (1 ng/ml) or G-CSF (10 ng/ml). Proliferative activity was measured by ^{3}H-thymidine incorporation. **(C):** Survival of neutrophils due to G-CSF stimulation. Neutrophils from the peritoneal cavity were cultured in IMDM supplemented with 10% FCS and 10 ng/ml G-CSF. Apoptosis of neutrophils was examined by flow cytometry after staining with PI and FITC-conjugated Gr1 on day 2. **(D):** Prevention of apoptosis of neutrophils in response to G-CSF. Neutrophils from the peritoneal cavity were cultured in IMDM supplemented with 10% FCS and 10 ng/ml G-CSF. Cell viability was determined by the trypan blue exclusion assay on the indicated days. Abbreviations: CFU-GM, colony-forming unit-granulocyte, macrophage; FCS, fetal calf serum; FITC, fluorescein isothiocyanate; IL, interleukin; IMDM, Iscove's modified Dulbecco's medium; PI, propidium iodide.

an increased number of apoptotic neutrophils (21%) from wild-type mice. In contrast, almost all of the neutrophils from Stat3-deficient mice were protected from apoptosis (Fig. 2C). Consistent with this observation, the survival of Stat3-deficient neutrophils was enhanced in culture with G-CSF (especially after a 2-day incubation) (Fig. 2D).

Stat3 Deficiency Enhances the Mobilization of Hematopoietic Progenitor Cells into the Peripheral Blood after In Vivo Administration of G-CSF

To assess the role of Stat3 in the G-CSF signaling pathway, we first treated mice with pIpC and then, after 14 days, treated them with daily injections of G-CSF for 7 days. After G-CSF treatment, the number of neutrophils was measured. Control littermates responded to G-CSF, and the number of peripheral blood neutrophils increased. Mx1:Stat3$^{flox/-}$ mice also responded to G-CSF, and the number of neutrophils after G-CSF treatment was almost the same in both cases (Fig. 3A). In addition to increasing the number of mature neutrophils in the peripheral blood, G-CSF also mobilizes hematopoietic progenitor cells from the bone marrow into the peripheral blood. Before treatment with G-CSF, no colony-forming hematopoietic progenitor cells were found in the peripheral blood (data not shown). In vivo G-CSF administration to control mice mobilized hematopoietic progenitor cells into the peripheral blood; this phenomenon could be assessed by colony-forming assay. In Mx1:Stat3$^{flox/-}$ mice, the number of hematopoietic progenitor cells mobilized by G-CSF was increased compared with the number mobilized in control mice (Fig. 3B).

However, the chemotactic activity of neutrophils toward fMLP was almost identical in wild-type and Stat3-deficient cells (Fig. 3C).

In addition to G-CSF, TPO also activates Stat3 in hematopoietic cells. Administration of TPO for 5 days increased the number of platelets in mice, and the deletion of Stat3 in hematopoietic cells did not alter this effect (Fig. 3D).

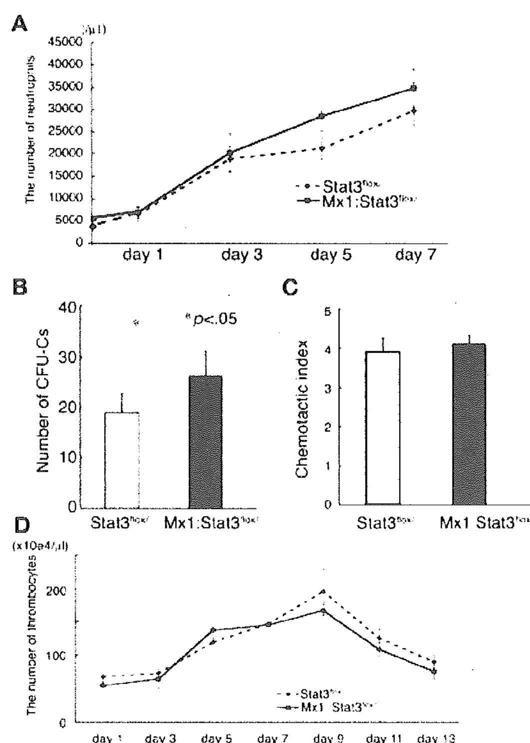

Figure 3. (A): In vivo administration of G-CSF. Stat3$^{flox/-}$ and Mx1:Stat3$^{flox/-}$ mice were injected subcutaneously with G-CSF from days 1 through 7 at 50 μg/kg. Peripheral blood was collected on the indicated day, 6 hours after G-CSF injection. **(B):** Mobilization of progenitor cells after administration of G-CSF in vivo. Stat3$^{flox/-}$ and Mx1:Stat3$^{flox/-}$ mice ($n = 5$) were injected subcutaneously with G-CSF from days 1 through 5 at 50 μg/kg. At day 5, peripheral blood mononuclear cells (2×10^5 cells/plate) were plated in methylcellulose containing interleukin-3 (20 ng/ml), stem cell factor (20 ng/ml), and erythropoietin (4 U/ml). The number of mobilized progenitor cells (CFU-C) was measured after 10 days in culture. **(C):** Chemotactic activity of neutrophils. Neutrophils from the peritoneal cavity were placed in the upper chamber and were attracted by fMLP in the lower chamber for 1 hour. The cells that passed through the membrane were counted, and the results are shown as the chemotactic index. **(D):** In vivo administration of TPO. Stat3$^{flox/-}$ and Mx1:Stat3$^{flox/-}$ mice were injected intraperitoneally with TPO from days 1 through 5 at 30 μg/kg. Peripheral blood was collected at the indicated day, 6 hours after TPO injection. Abbreviations: CFU-C, colony-forming unit-culture; TPO, thrombopoietin.

Stat3-Deficient Mice Develop Enterocolitis and Are Susceptible to DSS-Induced Colitis

Because mice with conditional deletion of Stat3 in macrophages and neutrophils (generated using LysM-Cre) developed colitis [26] and mice with conditional deletion of Stat3 in the bone marrow and endothelial cells (generated using Tie2-Cre) developed Crohn's-like disease [33], we performed histological analysis on the Mx1cre:Stat3$^{flox/-}$ mice 2 weeks after pIpC treatment. This histological analysis demonstrated a reduction in goblet cell number, inflammatory cells infiltrating the lamina propria, and formation of crypt abscesses (Fig. 4A). Neutrophils and monocytes infiltrated the submucosal, muscular, and serosa layers. These observations indicate that Stat3 deficiency in hematopoietic lineages enhanced inflammation in the intestine.

Next we investigated the role of Stat3 in an experimental inflammatory bowel disease model, DSS-induced colitis. Seven days after DSS administration, Mx1:Stat3$^{flox/-}$ mice developed severe colitis characterized by loss of weight (Fig. 4B), extensive leukocyte infiltration, and necrosis of the lamina propria (Fig. 4A). These changes were also observed in control mice, but the degree of weight loss and inflammation were extremely mild compared with the Mx1:Stat3$^{flox/-}$ mice. Two of five Mx1:Stat3$^{flox/-}$ mice after DSS administration died, whereas all of the control mice survived. These data suggest that Stat3 plays a negative regulatory role in intestinal inflammation.

Absence of SOCS3 Induction by G-CSF in Stat3-Deficient Bone Marrow Cells

The cytokine signaling is negatively regulated by SOCS family protein. Among them, SOCS3 is induced by G-CSF, and SOCS3 binds to phosphorylated G-CSR receptors to prevent Jak kinase activation. As shown in Figure 5, SOCS3 was induced by G-CSF stimulation in bone marrow cells from wild-type mice. By contrast, the expression level of SOCS3 protein in Stat3-deficient bone marrow cells is a trace, and it is not augmented by G-CSF stimulation.

Enhanced ERK Phosphorylation in Stat3-Deficient Bone Marrow Cells

Neutrophilia and colitis are observed in mice with conditional deletion of Stat3 in hematopoietic cells. G-CSF is the main cytokine regulating the proliferation and differentiation of cells in the granulocyte lineage [1], and the binding of G-CSF to its receptor activates the Ras–mitogen-activated protein kinase (MAPK) signaling cascade and the Jak-Stat signaling pathway [13, 14]. Therefore, we examined the intracellular signaling pathways induced by G-CSF. In bone marrow cells from control mice, G-CSF stimulation promptly activated extracellular regulated kinase 1

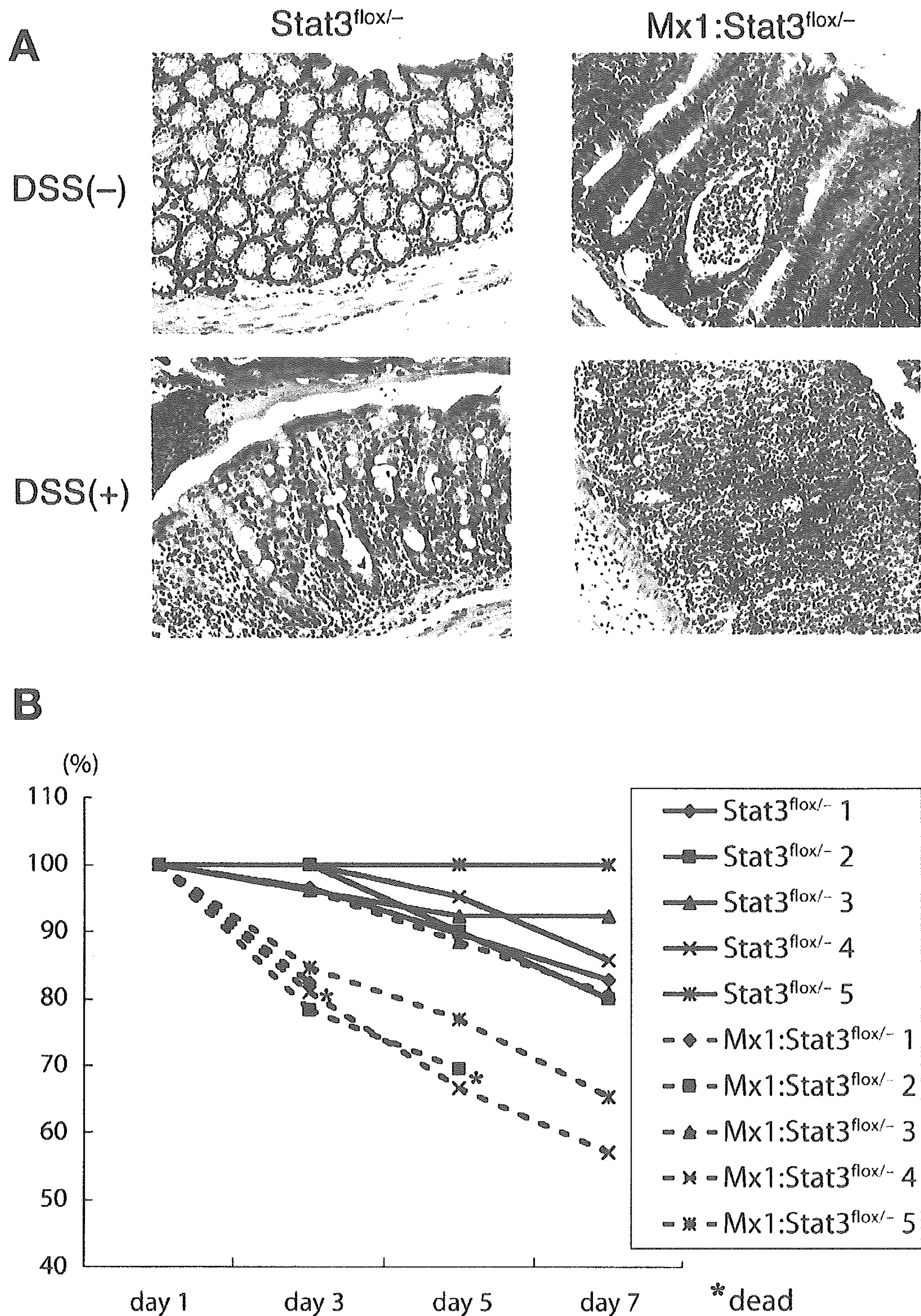

Figure 4. (A): Histological analysis of colitis. $Stat3^{flox/-}$ and $Mx1:Stat3^{flox/-}$ mice were treated with or without 4% DSS for 7 days. At day 7, mice were euthanized, and histological analysis was performed. Histological sections of the colon were stained with hematoxylin and eosin. Magnification ×200. **(B):** Time course of DSS-induced body weight loss. $Stat3^{flox/-}$ and $Mx1:Stat3^{flox/-}$ mice (n = 5) were treated with 4% DSS for 7 days, and body weight was measured at the indicated day. Relative body weight compared with the day-1 baseline was plotted. Abbreviation: DSS, dextran sulfate sodium.

(ERK1)/ERK2, and the activation diminished 60 minutes after stimulation (Fig. 6A). Stat3 activation occurred 30 minutes after G-CSF stimulation and was still apparent 120 minutes after G-CSF stimulation. In bone marrow cells from Mx1: Stat3$^{flox/-}$ mice 14 days after pIpC treatment, G-CSF–induced activation of Stat3 did not occur. However, ERK phosphorylation was observed in the absence of G-CSF stimulation. Furthermore, G-CSF stimulation increased the already high basal levels of ERK phosphorylation, and the activation was prolonged until 120 minutes after stimulation (Fig. 6A).

ERK1/2 is autonomously activated in bone marrow cells with specific deletion of Stat3; therefore, it is possible that the G-CSF–mediated hyperproliferation in Stat3-deficient bone marrow cells is attributable to the augmented activation of MAPK. We next examined the effects of MAPK activation on the G-CSF–mediated proliferation of bone marrow cells. G-CSF induced the proliferation of bone marrow cells from control mice, and the MEK kinase inhibitor U0126 almost completely inhibited this proliferative activity (Fig. 6B). Stat3-deficient bone marrow cells showed an enhanced proliferative activity after G-CSF treatment compared with wild-type cells. A large part of the augmented proliferative activity induced by G-CSF in Stat3-deficient bone marrow cells was abolished by the addition of U0126. These data indicate that MAPK activation is responsible for most of the enhanced proliferative activity of G-CSF–stimulated Stat3-deficient bone marrow cells. Furthermore, the activation of Stat3 by G-CSF negatively regulates the MAPK activation.

Discussion

G-CSF specifically stimulates the proliferation and differentiation of cells that are committed to the neutrophil-granulocyte lineage. Because mice lacking G-CSF or the G-CSF receptor had impaired production of mature granulocytes [34, 35], G-CSF is thought to be the major regulator of differentiation and activation in the granulocyte lineage. The binding of G-CSF to the G-CSF receptor induced activation of the Jak-Stat pathway [3–6, 10, 11] and the Ras-Raf-ERK pathway [10, 11]. In the Jak-Stat pathway, Jak1, Jak2, Tyk2, Stat1, Stat3, and Stat5 are tyrosine phosphorylated in response to G-CSF [3–6, 10, 11]. Among the Stats, Stat3 is mainly tyrosine phosphorylated [4, 10], and transgenic mice with a targeted mutation of the G-CSF receptor (d715F) that abrogates Stat3 activation have granulopenia [24]. We now report the generation of mice lacking Stat3 in the hematopoietic system to analyze Stat3 functions in vivo.

Although mice lacking G-CSF or the G-CSF receptor showed a decrease in peripheral neutrophils [34, 35], mice with the Stat3 deficiency in the hematopoietic system do not have neutropenia. Rather, these mice have granulocytosis, consistent with the result reported by Welte et al. [33] or Lee et al. [36]. Furthermore, the number of neutrophils in

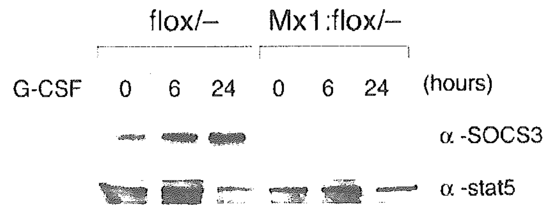

Figure 5. Induction of the SOCS3 protein in response to G-CSF stimulation of bone marrow cells from Stat3$^{flox/-}$ and Mx1: Stat3$^{flox/-}$ mice. Bone marrow cells from Stat3$^{flox/-}$ and Mx1: Stat3$^{flox/-}$ mice were incubated for 8 hours in the absence of G-CSF and were then stimulated with G-CSF (50 ng/ml) for the indicated period. Total cell lysates were analyzed by Western blot with the indicated antibodies.

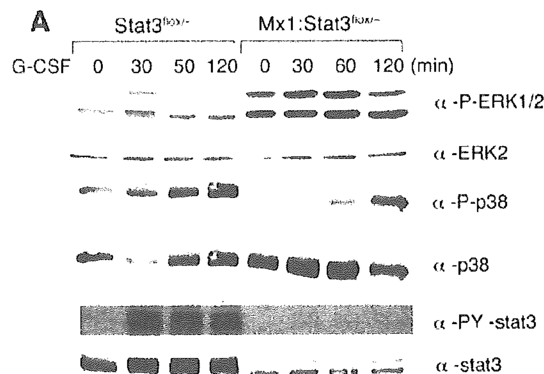

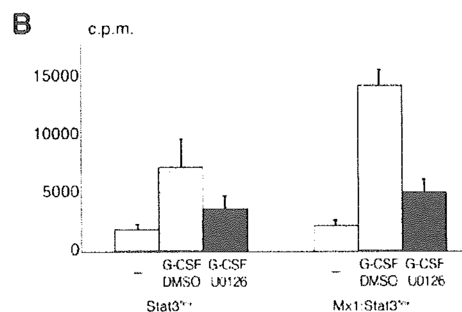

Figure 6. (A): Phosphorylation of ERK1/2 in response to G-CSF stimulation of bone marrow cells from Stat3$^{flox/-}$ and Mx1: Stat3$^{flox/-}$ mice. Bone marrow cells from Stat3$^{flox/-}$ and Mx1: Stat3$^{flox/-}$ mice were incubated for 8 hours in the absence of G-CSF and were then stimulated with G-CSF (50 ng/ml) for the indicated period. Total cell lysates were analyzed by Western blot with the indicated antibodies. **(B):** Inhibition of G-CSF–mediated proliferative activity by the MEK1/2 inhibitor U0126. Bone marrow cells (1×10^6/ml) were incubated for 3 days in the presence of G-CSF (10 ng/ml) with 1 μM of the MEK1/2 inhibitor U0126 or DMSO. Proliferative activity was measured by ^{3}H-thymidine incorporation. Abbreviations: DMSO, dimethyl sulfoxide; ERK, extracellular regulated kinase.

the bone marrow was greater in mice deficient for Stat3 in the hematopoietic system (Fig. 1B). There was no difference in the number of progenitor cells (CFU-G, CFU-GM) in the bone marrow between wild-type mice and mice deficient for Stat3 in the hematopoietic system, as assessed by the number of colony-forming cells (Fig. 2A). Therefore, we next examined the proliferative response of bone marrow cells to G-CSF stimulation. As shown in Figure 2B, bone marrow cells from the mice deficient for Stat3 in the hematopoietic system responded more strongly to G-CSF stimulation than cells from wild-type mice. Furthermore, apoptosis in cultures supplemented with G-CSF was suppressed by ablation of Stat3 in neutrophils (Fig. 2C). Thus, the enhanced proliferation of neutrophils observed in mice deficient for Stat3 in the hematopoietic system is attributable both to the augmented proliferation of neutrophilic progenitor cells in response to G-CSF and prolonged neutrophil survival in response to G-CSF.

The G-CSF–induced mobilization of hematopoietic progenitor cells from the bone marrow into the peripheral blood is also augmented by the absence of Stat3 in hematopoietic cells (Fig. 3B). The mechanism by which hematopoietic progenitor cells are mobilized from the bone marrow into the peripheral blood in response to G-CSF has not been elucidated. G-CSF causes neutrophils to secrete proteases, which allows hematopoietic progenitor cells to release from the bone marrow microenvironment into the peripheral blood. Because the absence of Stat3 in hematopoietic cells had no effect on the number of hematopoietic progenitor cells in the bone marrow (Fig. 2A), the augmented mobilization induced by G-CSF in Stat3-deficient mice must be attributable to hyperactivity of the Stat3-deficient neutrophils in response to G-CSF stimulation. On the other hand, the fMLP-induced chemotactic activity of neutrophils was not affected by the absence of Stat3 in neutrophils (Fig. 3C).

We assessed the presence of pathological abnormalities caused by the deletion of Stat3 in the hematopoietic system. There was some infiltration of inflammatory cells into the mucosa propria in the stomach and small intestine (data not shown), and moderate inflammation and the disappearance of goblet cells were observed in the colon (Fig. 4A). No inflammation was observed in the brain, liver, or lung. Welte et al. [33] also reported that pathological abnormalities similar to those observed in Crohn's disease occurred in mice with conditional deletion of Stat3 driven by the Tie2 promoter (Stat3CFF) [33]. Stat3CFF mice had widespread inflammatory disease in the digestive tract, and close to 100% of the animals died by 4–6 weeks after birth. Although our Stat3-deficient mice developed colitis, they survived under specific pathogen-free conditions. Because Tie-2 is expressed in hemangioblasts [37], the deletion of Stat3 in the blood vessels may lead to severe inflammation in the digestive tract.

Conditional knockout of Stat3 in macrophages and neutrophils resulted in chronic enterocolitis with age [26]. Mice deficient for Stat3 in hematopoietic cells developed colitis in their youth. Thus, the deletion of Stat3 not only in mature neutrophils and macrophages but also in immature myeloid cells might augment the development of colitis.

We next investigated the role of Stat3 in the pathology of DSS-induced colitis. Stat3 is mainly activated by G-CSF, IL-6, and IL-10, and elevation of IL-6 levels has been reported in DSS-induced colitis. The degree of emaciation after DSS treatment is more severe in mice lacking Stat3 in hematopoietic cells than in control mice, and two of five Stat3-deficient mice died during DSS administration (Fig. 4B). After DSS treatment, the disappearance of the gland duct, necrosis of the proper mucosa, and infiltration of inflammatory cells into the serosa were observed in mice deficient for Stat3 in the hematopoietic system, although moderate infiltration also occurred in wild-type mice (Fig. 4A). The deletion of Stat3 in hematopoietic cells augmented the infiltration of inflammatory cells into the digestive tract in DSS-induced colitis. Taken together, these data indicate that the ablation of Stat3 in hematopoietic cells enhanced the response (proliferation and inflammation) to cytokines, including G-CSF, which is likely due to the loss of negative regulatory signals.

The suppressor of cytokine signaling (SOCS) family is a group of negative regulators of cytokine signaling [38–42]. These proteins are induced as part of the cellular response to cytokines. In particular, SOCS3 expression is induced by G-CSF stimulation [43]. SOCS3 binds selectively to phosphorylated tyrosine residues in the G-CSF receptor (Y729 in human and Y728 in murine G-CSF receptor) through its SH2 domain and inhibits the catalytic activity of Jaks [43]. Therefore, we examined whether the expression level of SOCS3 was affected by the deletion of Stat3 in hematopoietic cells. Only trace levels of SOCS3 were expressed in bone marrow cells from mice deficient for Stat3 in the hematopoietic system, and this expression was not induced by G-CSF stimulation. In contrast, G-CSF treatment induced the expression of SOCS3 in bone marrow cells from wild-type mice (Fig. 5). Taken together, these data indicate that Stat3 is required for induction of SOCS3 in response to G-CSF signaling. Furthermore, the absence of SOCS3 negative feedback may allow prolonged Jak activation, resulting in enhanced signaling and increased proliferation. Certainly the phenotype of mice deficient for SOCS3 in hematopoietic cells [44, 45] is extremely similar to the phenotype of mice deficient for Stat3 in hematopoietic cells. SOCS3-deficient mice developed neutrophilia, and cells from the neutrophil-granulocyte lineage of mice deficient for SOCS3 in hematopoietic cells displayed an enhanced cellular response to in vitro stimulation with G-CSF.

Stat3 is the principal protein activated by G-CSF [6, 10]. 32Dcl3 cells normally differentiate into neutrophils after treatment with G-CSF; however, when these cells express dominant-negative Stat3 (32Dcl3/DNStat3), they proliferate in the presence of G-CSF, but they maintain immature morphologic characteristics without evidence of differentiation [23]. Additionally, transgenic mice with a targeted mutation in the G-CSF receptor, which abolishes G-CSF–dependent Stat3 activation, have severe neutropenia with an accumulation of immature myeloid precursors in the bone marrow [24]. These data suggest that Stat3 transduces the differentiation signal of G-CSF. However, our study clearly shows that Stat3 actually transduces an inhibitory signal by the induction of SOCS3 in response to G-CSF signaling. This observation led us to ask what molecule transduces the proliferation and differentiation signals of G-CSF. G-CSF is known to activate Stat1 and Stat5, each of which might be involved in regulating cell proliferation. However, the deletion of Stat1 does not affect granulopoiesis [18]. The Stat5a/Stat5b double-knockout mouse has normal levels of neutrophils and monocytes, although G-CSF–stimulated colony formation of bone marrow cells is slightly affected by the absence of both Stat5a and Stat5b [21]. These phenotypes, together with the phenotype of mice deficient for Stat3 in the hematopoietic system, strongly suggest that ERK is a plausible candidate as a downstream mediator of G-CSF signaling responsible for proliferation and differentiation. This is consistent with a recent report indicating that Tyr-764 of the G-CSF receptor is the most important element for G-CSF–induced proliferation, which was reversed by inhibition of ERK activity [46].

Therefore, we evaluated the role of MAPK in the G-CSF signaling pathway (Figs. 6A, 6B). Wild-type bone marrow cells displayed a transient activation of ERK1/2 after G-CSF stimulation. In contrast, Stat3-null bone marrow cells displayed a significant activation of ERK1/2 even under basal conditions. In these cells, ERK activation was enhanced by G-CSF stimulation, and it was more sustained, remaining significantly elevated 60 minutes after G-CSF stimulation (Fig. 6A). Because enhanced proliferation of granulocytes in response to G-CSF in Stat3-null cells might result from the enhanced and prolonged activation of ERK, we studied the effects of the MEK1 inhibitor U0126, which blocks activation of ERK1 and ERK2, on G-CSF–induced proliferation of wild-type and Stat3-deficient bone marrow cells. As shown in Figure 6B, addition of U0126 to the cultures inhibited G-CSF–induced cell proliferation in wild-type mice. Surprisingly, the proliferative activity of Stat3-deficient bone marrow cells in response to G-CSF was dramatically decreased upon addition of U0126. These data indicate that MAPK activation is responsible for most of the proliferative activity of hematopoietic cells in response to G-CSF.

Acknowledgments

We would like to thank M. Sato and M. Ito for their excellent technical assistance and Drs. A. Nonami and A. Kimura (Kyushu University) for discussion. This work was supported in part by a grant from the Japanese Leukemia Foundation, a Grant for Clinical Research, and Grants-in-Aid for Scientific Research (13218096 and 15390302) from the Ministry of Education, Culture, Sports, Science, and Technology of Japan.

References

1 Demetri GD, Griffin JD. Granulocyte colony-stimulating factor and its receptor. Blood 1991;78:2791–2808.

2 Shimoda K, Okamura S, Harada N et al. High-frequency granuloid colony-forming ability of G-CSF receptor possessing CD34 antigen positive human umbilical cord blood hematopoietic progenitors. Exp Hematol 1995;23:226–228.

3 Nicholson SE, Oates AC, Harpur AG et al. Tyrosine kinase JAK1 is associated with the granulocyte-colony-stimulating factor receptor and both become tyrosine-phosphorylated after receptor activation. Proc Natl Acad Sci U S A 1994;91:2985–2988.

4 Nicholson SE, Novak U, Ziegler SF et al. Distinct regions of the granulocyte colony-stimulating factor receptor are required for tyrosine phosphorylation of the signaling molecules JAK2, Stat3, and p42, p44MAPK. Blood 1995;86:3698–3704.

5 Shimoda K, Iwasaki H, Okamura S et al. G-CSF induces tyrosine phosphorylation of the JAK2 protein in the human myeloid G-CSF responsive and proliferative cells, but not in mature neutrophils. Biochem Biophys Res Commun 1994;203:922–928.

6 Shimoda K, Feng J, Murakami H et al. Jak1 plays an essential role for receptor phosphorylation and Stat activation in response to granulocyte colony-stimulating factor. Blood 1997;90:597–604.

7 Ihle JN. Cytokine receptor signalling. Nature 1995;377:591–594.

8 Ihle JN, Nosaka T, Thierfelder W et al. Jaks and Stats in cytokine signaling. STEM CELLS 1997;15(suppl 1):105–111.

9 Ihle JN. STATs: signal transducers and activators of transcription. Cell 1996;84:331–334.

10 Tian SS, Lamb P, Seidel HM et al. Rapid activation of the STAT3 transcription factor by granulocyte colony-stimulating factor. Blood 1994;84:1760–1764.

11 de Koning JP, Dong F, Smith L et al. The membrane-distal cytoplasmic region of human granulocyte colony-

stimulating factor receptor is required for STAT3 but not STAT1 homodimer formation. Blood 1996:87:1335–1342.

12 Darnell JE Jr, Kerr IM, Stark GR. Jak-STAT pathways and transcriptional activation in response to IFNs and other extracellular signaling proteins. Science 1994;264:1415–1421.

13 Corey SJ, Burkhardt AL, Bolen JB et al. Granulocyte colony-stimulating factor receptor signaling involves the formation of a three-component complex with Lyn and Syk protein-tyrosine kinases. Proc Natl Acad Sci U S A 1994; 91:4683–4687.

14 Matsuda T, Hirano T. Association of p72 tyrosine kinase with Stat factors and its activation by interleukin-3, interleukin-6, and granulocyte colony-stimulating factor. Blood 1994;83:3457–3461.

15 Rodig SJ, Meraz MA, White JM et al. Disruption of the Jak1 gene demonstrates obligatory and nonredundant roles of the Jaks in cytokine-induced biologic responses. Cell 1998;93:373–383.

16 Shimoda K, Kato K, Aoki K et al. Tyk2 plays a restricted role in IFN alpha signaling, although it is required for IL-12-mediated T cell function. Immunity 2000:13:561–571.

17 Parganas E, Wang D, Stravopodis D et al. Jak2 is essential for signaling through a variety of cytokine receptors. Cell 1998:93:385–395.

18 Meraz MA, White JM, Sheehan KC et al. Targeted disruption of the Stat1 gene in mice reveals unexpected physiologic specificity in the JAK-STAT signaling pathway. Cell 1996;84:431–442.

19 Shimoda K, van Deursen J, Sangster MY et al. Lack of IL-4-induced Th2 response and IgE class switching in mice with disrupted Stat6 gene. Nature 1996:380:630–633.

20 Thierfelder WE, van Deursen JM, Yamamoto K et al. Requirement for Stat4 in interleukin-12-mediated responses of natural killer and T cells. Nature 1996;382:171–174.

21 Teglund S, McKay C, Schuetz E et al. Stat5a and Stat5b proteins have essential and nonessential, or redundant, roles in cytokine responses. Cell 1998:93:841–850.

22 Takeda K, Tanaka T, Shi W et al. Essential role of Stat6 in IL-4 signalling. Nature 1996;380:627–630.

23 Nakajima H, Ihle JN. Granulocyte colony-stimulating factor regulates myeloid differentiation through CCAAT/enhancer-binding protein epsilon. Blood 2001;98:897–905.

24 McLemore ML, Grewal S, Liu F et al. STAT-3 activation is required for normal G-CSF-dependent proliferation and granulocytic differentiation. Immunity 2001:14:193–204.

25 Takeda K, Noguchi K, Shi W et al. Targeted disruption of the mouse *Stat3* gene leads to early embryonic lethality. Proc Natl Acad Sci U S A 1997;94:3801–3804.

26 Takeda K, Clausen BE, Kaisho T et al. Enhanced Th1 activity and development of chronic enterocolitis in mice devoid of Stat3 in macrophages and neutrophils. Immunity 1999:10:39–49.

27 Takeda K, Kaisho T, Yoshida N et al. Stat3 activation is responsible for IL-6-dependent T cell proliferation through preventing apoptosis: generation and characterization of T cell-specific Stat3-deficient mice. J Immunol 1998:161:4652–4660.

28 Kuhn R, Schwenk F, Aguet M et al. Inducible gene targeting in mice. Science 1995:269:1427–1429.

29 Ludwig A, Petersen F, Zahn S et al. The CXC-chemokine neutrophil-activating peptide-2 induces two distinct optima of neutrophil chemotaxis by differential interaction with interleukin-8 receptors CXCR-1 and CXCR-2. Blood 1997:90:4588–4597.

30 Kato K, Kamezaki K, Shimoda K et al. Intracellular signal transduction of interferon on the suppression of haematopoietic progenitor cell growth. Br J Haematol 2003;123:528–535.

31 Kanauchi O, Nakamura T, Agata K et al. Effects of germinated barley foodstuff on dextran sulfate sodium-induced colitis in rats. J Gastroenterol 1998:33:179–188.

32 Aoki K, Shimoda K, Oritani K et al. Limitin, an interferon-like cytokine, transduces inhibitory signals on B-cell growth through activation of Tyk2, but not Stat1, followed by induction and nuclear translocation of Daxx. Exp Hematol 2003;31:1317–1322.

33 Welte T, Zhang SS, Wang T et al. STAT3 deletion during hematopoiesis causes Crohn's disease-like pathogenesis and lethality: a critical role of STAT3 in innate immunity. Proc Natl Acad Sci U S A 2003:100:1879–1884.

34 Lieschke GJ, Grail D, Hodgson G et al. Mice lacking granulocyte colony-stimulating factor have chronic neutropenia, granulocyte and macrophage progenitor cell deficiency, and impaired neutrophil mobilization. Blood 1994;84:1737–1746.

35 Liu F, Wu HY, Wesselschmidt R et al. Impaired production and increased apoptosis of neutrophils in granulocyte colony-stimulating factor receptor-deficient mice. Immunity 1996;5:491–501.

36 Lee CK, Raz R, Gimeno R et al. STAT3 is a negative regulator of granulopoiesis but is not required for G-CSF-dependent differentiation. Immunity 2002;17:63–72.

37 Maisonpierre PC, Suri C, Jones PF et al. Angiopoietin-2, a natural antagonist for Tie2 that disrupts in vivo angiogenesis. Science 1997;277:55–60.

38 Endo TA, Masuhara M, Yokouchi M et al. A new protein containing an SH2 domain that inhibits JAK kinases. Nature 1997:387:921–924.

39 Kamura T, Sato S, Haque D et al. The Elongin BC complex interacts with the conserved SOCS-box motif present in members of the SOCS, ras, WD-40 repeat, and ankyrin repeat families. Genes Dev 1998:12:3872–3881.

40 Naka T, Narazaki M, Hirata M et al. Structure and function of a new STAT-induced STAT inhibitor. Nature 1997;387:924–929.

41 Starr R, Willson TA, Viney EM et al. A family of cytokine-inducible inhibitors of signalling. Nature 1997:387:917–921.

42 Sasaki A, Yasukawa H, Suzuki A et al. Cytokine-inducible SH2 protein-3 (CIS3/SOCS3) inhibits Janus tyrosine kinase by binding through the N-terminal kinase inhibitory region as well as SH2 domain. Genes Cells 1999:4:339–351.

43 Hortner M, Nielsch U, Mayr LM et al. Suppressor of cytokine signaling-3 is recruited to the activated granulocyte-colony stimulating factor receptor and modulates its signal transduction. J Immunol 2002;169:1219–1227.

44 Kimura A, Kinjyo I, Matsumura Y et al. SOCS3 is a physiological negative regulator for granulopoiesis and granulocyte colony-stimulating factor receptor signaling. J Biol Chem 2004;279:6905–6910.

45 Croker BA, Metcalf D, Robb L et al. SOCS3 is a critical physiological negative regulator of G-CSF signaling and emergency granulopoiesis. Immunity 2004;20:153–165.

46 Hermans MH, van de Geijn GJ, Antonissen C et al. Signaling mechanisms coupled to tyrosines in the granulocyte colony-stimulating factor receptor orchestrate G-CSF-induced expansion of myeloid progenitor cells. Blood 2003;101:2584–2590.

Development of functional human blood and immune systems in NOD/SCID/IL2 receptor γ chain^{null} mice

Fumihiko Ishikawa, Masaki Yasukawa, Bonnie Lyons, Shuro Yoshida, Toshihiro Miyamoto, Goichi Yoshimoto, Takeshi Watanabe, Koichi Akashi, Leonard D. Shultz, and Mine Harada

Here we report that a new nonobese diabetic/severe combined immunodeficient (NOD/SCID) mouse line harboring a complete null mutation of the common cytokine receptor γ chain (NOD/SCID/interleukin 2 receptor [IL2r] γ^{null}) efficiently supports development of functional human hemato-lymphopoiesis. Purified human (h) CD34^{+} or hCD34^{+}hCD38^{-} cord blood (CB) cells were transplanted into NOD/SCID/IL2rγ^{null} newborns via a facial vein. In all recipients injected with 10^5 hCD34^{+} or 2×10^4 hCD34^{+}hCD38^{-} CB cells, human hematopoietic cells were reconstituted at approximately 70% of chimerisms. A high percentage of the human hematopoietic cell chimerism persisted for more than 24 weeks after transplantation, and hCD34^{+} bone marrow grafts of primary recipients could reconstitute hematopoiesis in secondary NOD/SCID/IL2rγ^{null} recipients, suggesting that this system can support self-renewal of human hematopoietic stem cells. hCD34^{+}hCD38^{-} CB cells differentiated into mature blood cells, including myelomonocytes, dendritic cells, erythrocytes, platelets, and lymphocytes. Differentiation into each lineage occurred via developmental intermediates such as common lymphoid progenitors and common myeloid progenitors, recapitulating the steady-state human hematopoiesis. B cells underwent normal class switching, and produced antigen-specific immunoglobulins (Igs). T cells displayed the human leukocyte antigen (HLA)–dependent cytotoxic function. Furthermore, human IgA-secreting B cells were found in the intestinal mucosa, suggesting reconstitution of human mucosal immunity. Thus, the NOD/SCID/IL2rγ^{null} newborn system might be an important experimental model to study the human hemato-lymphoid system. (Blood. 2005;106:1565-1573)

© 2005 by The American Society of Hematology

Introduction

To analyze human immune and hematopoietic development and function in vivo, a number of studies have been tried to reproduce human hematopoiesis in small animal xenotransplantation models.[1] Successful transplantation of human hematopoietic tissues in immune-compromised mice was first reported in late 1980s by using homozygous severe combined immunodeficient (C.B.17-SCID) mice. In the first model of a humanized lymphoid system in a SCID mouse (SCID-hu model), McCune et al simultaneously transplanted human fetal tissues, including fetal liver hematopoietic cells, thymus, and lymph nodes, into SCID mice and induced mature human T- and B-cell development.[2] Mosier et al successfully reconstituted human T and B cells by transferring human blood mononuclear cells into SCID mice.[3] These initial studies suggested the usefulness of immunodeficient mice for reconstitution of the human lymphoid system from human bone marrow hematopoietic stem cells (HSCs).

After these initial reports, a number of modified SCID models have been proposed to try to reconstitute human immunity.[4] In addition, recombination activating gene (RAG)–deficient strains have been used as recipients in xenotransplantation: T- and B-cell–deficient *Prkdc^{scid}*, *Rag1$^{-/-}$*, or *Rag2$^{-/-}$* mutant mice[5-7] were capable of supporting engraftment of human cells. The engraftment levels in these models, however, were still low, presumably due to the remaining innate immunity of host animals.[1] Nonobese diabetic/severe combined immunodeficient (NOD/SCID) mice have been shown to support higher levels of human progenitor cell engraftment than BALB/c/SCID or C.B.17/SCID mice.[8] Levels of human cell engraftment were further improved by treating NOD/SCID mice with anti-asialo GM1 (ganglioside-monosialic acid) antibodies[9] that can abrogate natural killer (NK) cell activity. Recently, NOD/SCID mice harboring either a null allele at the β_2-microglobulin gene (NOD/SCID/$\beta 2m^{-/-}$)[10] or a truncated common cytokine receptor γ chain (γc) mutant lacking its cytoplasmic region (NOD/SCID/$\gamma_c^{-/-}$)[11,12] were developed. In these mice, NK- as well as T- and B-cell development and functions are disrupted, because β2m is necessary for major histocompatibility complex (MHC) class I–mediated innate immunity, and because γc (originally called IL-2Rγ chain) is an indispensable component

From the Department of Medicine and Biosystemic Science, Kyushu University Graduate School of Medical Sciences, Fukuoka, Japan; First Department of Internal Medicine, Ehime University School of Medicine, Shigenobu, Japan; The Jackson Laboratory, Bar Harbor, ME; Center for Cellular and Molecular Medicine, Kyushu University Hospital, Fukuoka, Japan; RIKEN for Allergy and Immunology, Yokohama, Japan; and the Department of Cancer Immunology and AIDS, Dana-Farber Cancer Institute, Boston, MA.

Submitted February 9, 2005; accepted April 7, 2005. Prepublished online as *Blood* First Edition Paper, May 26, 2005; DOI 10.1182/blood-2005-02-0516.

Supported by grants from Japan Society for Promotion of Science (F.I.); the Ministry of Education, Culture, Sports, Science and Technology of Japan (M.Y.); the Ministry of Health, Labor, and Welfare of Japan (M.H.); and National Institutes of Health grants A130389 and HL077642 (L.D.S.) and DK061320 (K.A.).

The online version of the article contains a data supplement.

Reprints: Koichi Akashi, Department of Cancer Immunology and AIDS, Dana-Farber Cancer Institute, 44 Binney St, no. 770, Boston, MA 02115; e-mail: koichi_akashi@dfci.harvard.edu; or Leonard D. Shultz, The Jackson Laboratory, 600 Main St, Bar Harbor, ME 04609.

The publication costs of this article were defrayed in part by page charge payment. Therefore, and solely to indicate this fact, this article is hereby marked "advertisement" in accordance with 18 U.S.C. section 1734.

© 2005 by The American Society of Hematology

of receptor heterodimers for many lymphoid-related cytokines (ie, IL-2, IL-7, IL-9, IL-12, IL-15, and IL-21).[13] Injection of human bone marrow or cord blood (CB) cells into these mice resulted in successful generation of human T and B cells. In our hands, efficiencies of CB cell engraftment represented by percentages of circulating human (h) $CD45^+$ cells were significantly (2- to 5-fold) higher in NOD/SCID/$\beta 2m^{-/-}$ newborns than those in adults (F.I., M.H., and L.D.S., unpublished data, April 2003). More recently, transplantation of $hCD34^+$ CB cells into $Rag2^{-/-}$ $\gamma c^{-/-}$ newborns regenerated adaptive immunity mediated by functional T and B cells,[14] suggesting heightened support for xenogeneic transplants especially in the neonatal period. Efficiency of reconstitution of human hematopoiesis may be, however, still suboptimal in these models because chimerisms of human cells are not stable in each experiment.[11,12,14] Furthermore, there is little information regarding reconstitution of human myeloerythroid components in these xenogeneic models.

Two types of mouse lines with truncated or complete null γc mutant[15-17] have been reported. NOD/SCID/$\gamma_c^{-/-}$ and $Rag2^{-/-}$ $\gamma c^{-/-}$ mouse strains harbor a truncated γc mutant lacking the intracellular domain,[15] and therefore, binding of γc-related cytokines to each receptor should normally occur in these models.[18] For example, IL-2R with the null γc mutations would be an αβ heterodimer complex with an affinity approximately 10 times lower than that of the high affinity αβγ heterotrimer complex in mice with the truncated γc mutant.[19] γc has also been shown to dramatically increase the affinity to its ligands through the receptors for IL-4, IL-7, and IL-15.[20-23] Previous studies suggested that γc-related receptors including IL-2Rβ chain and IL-4Rα chain could activate janus-activated kinases (JAKs) to some extent in the presence of the extracellular domain of γc, independent of the cytoplasmic domain of γc.[24,25] Thus, in order to block the signaling through γc-related cytokine receptors more completely, we made NOD/SCID mice harboring complete null mutation of γc[16] (the NOD/SCID/IL2$r\gamma^{null}$ strain). By using NOD/SCID/IL2$r\gamma^{null}$ newborns, we successfully reconstituted myeloerythroid as well as lymphoid maturation by injecting human CB or highly-enriched CB HSCs at a high efficiency. Reconstitution of human hematopoiesis persisted for a long term. The developing lymphoid cells were functional for immunoglobulin (Ig) production and human leukocyte antigen (HLA)–dependent cytotoxic activity. Our data show that the NOD/SCID/IL2$r\gamma^{null}$ newborn system provides a valuable tool to reproduce human hemato-lymphoid development.

Materials and methods

Mice

NOD.Cg-*Prkdc*^{scid}*Il2rg*^{tm1Wjl}/Sz (NOD/SCID/IL2$r\gamma^{null}$) and NOD/LtSz-*Prkdc*^{scid}/*B2m*^{null} (NOD/SCID/$\beta 2m^{null}$) mice were developed at the Jackson Laboratory (Bar Harbor, ME). The NOD/SCID/IL2$r\gamma^{null}$ strain was established by backcrossing a complete null mutation at γc locus[16] onto the NOD.Cg-*Prkdc*^{scid} strain. The establishment of this mouse line has been reported elsewhere.[26] All experiments were performed according to the guideline in the Institutional Animal Committee of Kyushu University.

Cell preparation and transplantation

CB cells were obtained from Fukuoka Red Cross Blood Center (Japan). CB cells were harvested after written informed consent. Mononuclear cells were depleted of Lin^+ cells using mouse anti-hCD3, anti-hCD4, anti-hCD8, anti-hCD11b, anti-hCD19, anti-hCD20, anti-hCD56, and anti–human glycophorin A (hGPA) monoclonal antibodies (BD Immunocytometry, San Jose, CA). Samples were enriched for $hCD34^+$ cells by using anti-hCD34 microbeads (Miltenyi Biotec, Auburn, CA). These cells were further stained with anti-hCD34 and hCD38 antibodies (BD Immunocytometry), and were purified for $Lin^-CD34^+CD38^-$ HSCs by a FACSVantage (Becton Dickinson, San Jose, CA). Lin^- $hCD34^+$ cells (10^5) or 2×10^4 $Lin^-hCD34^+hCD38^-$ cells were transplanted into irradiated (100 cGy) NOD/SCID/IL2$r\gamma^{null}$ or NOD/SCID/$\beta 2m^{null}$ newborns via a facial vein[27] within 48 hours of birth.

Examination of hematopoietic chimerism

At 3 months after transplantation, samples of peripheral blood, bone marrow, spleen, and thymus were harvested from recipient mice. Human common lymphoid progenitors were analyzed based on the expression of hCD127 (IL-7 receptor α chain) and hCD10 in Lin (hCD3, hCD4, hCD8, hCD11b, hCD19, hCD20, hCD56, and hGPA)$^-$ $hCD34^+hCD38^+$ fraction.[28,29] Human myeloid progenitors were analyzed based on the expressions of hCD45RA and hCD123 (IL-3 receptor α chain) in Lin^- $CD10^-CD34^+CD38^+$ fractions. For the analysis of megakaryocyte/erythroid (MegE) lineages, anti-hCD41a (HIP8), anti-hGPA (GAR-2), anti-mCD41a (MW Reg30), and anti-mTer119 (Ter-119) antibodies were used. Samples were treated with ammonium chloride to eliminate mature erythrocytes, and were analyzed by setting nucleated cell scatter gates. For the analysis of circulating erythrocytes and platelets, untreated blood samples were analyzed by setting scatter gates specific for each cell fraction. Human B lymphoid progenitors were evaluated according to the criteria proposed by LeBien.[30]

Methylcellulose culture assay

Bone marrow cells of recipient mice were stained with anti-hCD34, hCD38, hCD45RO, hCD123, and lineage antibodies. Human HSCs, CMPs, GMPs, and MEPs were purified according to the phenotypic definition[28,29] by using a FACSVantage (Becton Dickinson). One hundred cells of each population were cultured in methylcellulose media (Stem Cell Technologies, Vancouver, BC, Canada) supplemented with 10% bovine serum albumin (BSA), 20 μg/mL steel factor, 20 ng/mL IL-3, 20 ng/mL IL-11, 20 ng/mL Fms-like tyrosine kinase 3 (Flt3) ligand, 50 ng/mL granulocyte-macrophage colony-stimulating factor (GM-CSF), 4 U/ml erythropoietin (Epo), and 50 ng/mL thrombopoietin (Tpo). Colony numbers were enumerated on day 14 of culture.

Histologic analysis

Tissue samples were fixed with 4% paraformaldehyde and dehydrated with graded alcohol. After treatment with heated citrate buffer for antigen retrieval, paraformaldehyde-fixed paraffin-embedded sections were immunostained with mouse anti-hCD19, anti–human IgA, anti-hCD3, anti-hCD4, anti-hCD8, and anti-hCD11c antibodies (Dako Cytomation, Carpinteria, CA). Stained specimens were observed by confocal microscopy (LSM510 META microscope; Carl Zeiss, Oberkochen, Germany). Image acquisition and data analysis were performed by using LSM5 software. Numerical aperture of the objective lens (PlanApochromat ×63) used was 1.4.

ELISA

Human Ig concentration in recipient sera was measured by using a human immunoglobulin assay kit (Bethyl, Montgomery, IL). For detection of ovalbumin (OVA)–specific human IgM and IgG antibodies, 5 recipient mice were immunized twice every 2 weeks with 100 μg of OVA (Sigma, St Louis, MO) that were emulsified in aluminum hydroxide (Sigma). Sera from OVA-treated mice were harvested 2 weeks after the second immunization. OVA was plated at s concentration of 20 μg/mL on 96-microtiter wells at 4°C overnight. After washing and blocking with bovine serum albumin, serum samples were incubated in the plate for 1 hour. Antibodies binding OVA were then measured by a standard enzyme-linked immunosorbent assay (ELISA).

Cytotoxicity of alloantigen-specific human CD4+ and CD8+ T-cell lines

Alloantigen-specific human CD4+ and CD8+ T-cell lines were established according to the method as reported.[31] After stimulation with an Epstein Barr virus–transformed B lymphoblastoid cell line (TAK-LCL) established from a healthy individual (TAK-LCL) for 6 days, 100 hCD4+ T cells or hCD8+ T cells were plated with 3×10^4 TAK-LCL cells in the presence of 10 U/mL human IL-2 (Genzyme, Boston, MA), and were subjected to a chromium 51 (^{51}Cr) release assay. A Limiting number of effector cells and 10^4 ^{51}Cr-labeled allogeneic target cells were incubated. KIN-LCLs that do not share HLA with effector cells or TAK-LCL were used as negative controls. Cytotoxic activity was tested in the presence or absence of anti-HLA class I or anti–HLA-DR monoclonal antibodies.

Results

Reconstitution of human hematopoiesis is achieved in NOD/SCID/IL2rγ^{null} mice

NOD/SCID/IL2rγ^{null} mice lacked mature murine T or B cells evaluated by fluorescence-activated cell sorting (FACS), and displayed extremely low levels of NK cell activity.[31] This mouse line can survive more than 15 months[31] since it does not develop thymic lymphoma, usually a fatal disease in the immune-compromised mice with NOD background.[32]

Lin$^-$hCD34+ CB cells contain HSCs, and myeloid and lymphoid progenitors.[28,29] We and others have reported that engraftment of human CB cells, which contain hematopoietic stem and progenitor cells, was efficient in NOD/SCID/β2m$^{-/-}$ and RAG2$^{-/-}$/γ$_c^{-/-}$ mice, especially when cells were transplanted during the neonatal period.[14,33] We therefore transplanted purified Lin$^-$hCD34+ CB cells into sublethally irradiated NOD/SCID/IL2rγ^{null} newborns via a facial vein.[27]

We first transplanted 10^5 Lin$^-$hCD34+ CB cells from 3 independent donors into 5 NOD/SCID/IL2rγ^{null} newborns, and found that the NOD/SCID/IL2rγ^{null} newborn system is very efficient for supporting engraftment of human hematopoietic progenitor cells. Table 1 shows percentages of hCD45+ cells in these mice 3 months after transplantation. Strikingly, the average engraftment levels were approximately 70% in both the bone marrow and the peripheral blood. Compared with 4 control NOD/SCID/β2m$^{-/-}$ recipient mice given transplants from the same donors, engraftment levels of hCD45+ cells in NOD/SCID/IL2rγ^{null} mice were significantly higher (Table 1).

Table 1. Chimerism of human CD45+ cells in NOD/SCID/β2m^{null} mice and NOD/SCID/IL2rγ^{null} mice

	% nucleated cells		
Mouse no. (donor no.)	PB	BM	Spleen
NOD/SCID/IL2rγ^{null}			
1 (1)	71.2	70.9	66.8
2 (1)	81.7	81.4	47.1
3 (2)	50.1	58.8	49.5
4 (3)	68.0	83.1	51.1
5 (3)	73.3	70.1	58.1
Mean ± SD	68.9 ± 11.6*	72.9 ± 9.8*	54.5 ± 8.0*
NOD/SCID/β2m^{null}			
1 (1)	10.4	46.1	22.0
2 (2)	11.6	31.5	24.3
3 (3)	6.9	18.1	20.7
4 (3)	20.7	30.4	31.2
Mean ± SD	12.4 ± 5.9*	31.5 ± 11.5*	22.6 ± 4.7*

To compare the engraftment levels in the two strains, 1×10^5 Lin$^-$ CD34+ cells derived from 3 CB samples were transplanted into 5 NOD/SCID/IL2rγ^{null} mice and 4 NOD/SCID/β2m^{null} mice. At 3 months after transplantation, BM, spleen, and peripheral blood (PB) of the recipient mice were analyzed for the engraftment of human cells. Data show percentages of human CD45+ cells in each tissue.

*$P < .05$.

Table 2 shows the analysis of human hematopoietic cell progeny in mice that received transplants of human Lin$^-$hCD34+ CB cells. In the peripheral blood, hCD45+ cells included hCD33+ myeloid, hCD19+ B cells, and hCD3+ T cells in all mice analyzed (Figure 1A and Table 2). We then analyzed the reconstitution of erythropoiesis and thrombopoiesis in these mice. Anti–human glycophorin A (hGPA) antibodies recognized human erythrocytes, while mTer119 antibodies[34] recognized GPA-associated protein on murine erythrocytes, respectively (Figure 1B). Human and murine platelets could also be stained with anti–human and anti–murine CD41a, respectively (Figure 1B). Circulating hGPA+ erythrocytes and hCD41a+ platelets were detected in all 3 mice analyzed (Figure 1B, right panels). hGPA+ erythroblasts and hCD41a+ megakaryocytes were detected as 9.5% ± 6.2% (n = 5) and 1.64% ± 0.42% (n = 5) of nucleated bone marrow cells, respectively. Thus, transplanted human Lin$^-$hCD34+ CB cells differentiated into mature erythrocytes and platelets in NOD/SCID/IL2rγ^{null} recipients.

In all engrafted mice, the bone marrow and the spleen contained significant numbers of hCD11c+ dendritic cells as well as hCD33+ myeloid cells, hCD19+ B cells, and hCD3+ T cells (Table 2 and Figure 1C). hCD11c+ dendritic cells coexpressed HLA-DR that is essential for antigen presentation to T cells (Figure 1D). In contrast, in the thymus, the majority of cells were composed of hCD3+ T cells and rare hCD19+ B cells (Table 2).

Figure 2A shows the change in the percentage of circulating hCD45+ cells in another set of NOD/SCID/IL2rγ^{null} newborns injected with 2×10^4 Lin$^-$hCD34+hCD38$^-$ CB cells. Surprisingly, the level of hCD45+ cells in the blood was unchanged, and was maintained at a high level even 24 weeks after transplantation. Mice did not develop lymphoid malignancies or other complications. Furthermore, we tested the retransplantability of human HSCs in primary recipients. We killed mice at 24 weeks after the primary transplantation of hCD34+ cells, purified 1 to 5×10^4 hCD34+ cells from primary recipient bone marrow cells, and retransplanted them into NOD/SCID/IL2rγ^{null} newborns. In all 3 experiments, secondary recipients successfully reconstituted human hematopoiesis at least until 12 weeks after transplantation, when we killed mice for the bone marrow analysis (Figure 2B). Thus, the NOD/SCID/IL2rγ^{null} newborn system can support human hematopoiesis for the long term.

Human cord blood hematopoietic stem cells produced myeloid and lymphoid cells via developmental intermediates in the NOD/SCID/IL2rγ^{null} bone marrow

The Lin$^-$hCD34+ CB fraction contains early myeloid and lymphoid progenitors as well as HSCs.[28] To verify that differentiation into all hematopoietic cells can be initiated from human HSCs in the NOD/SCID/IL2rγ^{null} newborn system, we transplanted Lin$^-$hCD34+hCD38$^-$CB cells that contain the counterpart population of murine long-term HSCs,[35] and are highly enriched for human HSCs.[36,37] hCD34+ CB cells (15%-20%) were hCD38$^-$ (data not shown). Mice given transplants of 2×10^4 Lin$^-$hCD34+hCD38$^-$ cells displayed successful reconstitution of similar proportion of human cells compared with mice reconstituted with 1×10^5 Lin$^-$hCD34+ cells at 12 weeks after transplantation (Table 2). In another experiment, mice injected with 2×10^4 Lin$^-$hCD34+hCD38$^-$ cells exhibited the high chimerism (> 50%)

Table 2. Cellular number and composition in tissues of engrafted NOD/SCID/IL2rγ^{null} mice

Injected cells, mice, and tissue type	Total no. cells	% nucleated cells (% hCD45⁺ cells)			
		CD33	CD19	CD3	CD11c
1 × 10^5 Lin$^-$CD34$^+$					
Mouse no. 1/ donor no. 1					
BM	2.4 × 10^7	8.2 (11.6)	54.8 (77.6)	10.7 (15.1)	1.1 (1.6)
Spleen	4.1 × 10^7	4.3 (6.4)	33.5 (50.1)	26.1 (39.1)	2.2 (3.3)
Thymus	3.1 × 10^5	NE	1.3 (1.3)	96.2 (98.7)	NE
PB	NE	4.0 (5.6)	35.1 (49.3)	19.8 (27.8)	NE
Mouse no. 2/donor no. 1					
BM	1.8 × 10^7	5.5 (6.8)	56.5 (67.6)	9.9 (12.2)	2.9 (3.6)
Spleen	3.2 × 10^7	2.1 (4.5)	27.7 (58.8)	15.9 (33.8)	1.3 (2.8)
Thymus	4.5 × 10^5	NE	1.1 (1.2)	90.4 (98.8)	NE
PB	NE	6.1 (7.5)	53.8 (65.9)	21.6 (40.1)	NE
Mouse no. 4/ donor no. 3					
BM	1.9 × 10^7	9.4 (11.3)	52.9 (63.7)	15.9 (19.1)	0.62 (0.75)
Spleen	4.4 × 10^7	3.5 (6.8)	24.2 (47.4)	20.8 (40.7)	1.5 (2.9)
Thymus	0.8 × 10^5	NE	0.88 (1.1)	78.2 (98.9)	NE
PB	NE	3.2 (4.7)	61.3 (90.1)	5.3 (7.8)	NE
Mouse no. 5/donor no. 3					
BM	2.1 × 10^7	10.2 (14.6)	48.8 (82.0)	9.4 (13.4)	1.3 (1.9)
Spleen	2.7 × 10^7	6.6 (11.4)	30.4 (52.3)	18.6 (32.0)	1.1 (1.9)
Thymus	1.1 × 10^5	NE	3.1 (3.7)	81.1 (96.3)	NE
PB	NE	9.8 (13.4)	40.4 (55.1)	16.8 (22.9)	NE
2 × 10^4 Lin$^-$CD34$^+$CD38$^-$					
Mouse no. 6/donor no. 4					
BM	2.6 × 10^7	3.1 (5.3)	46.1 (78.7)	8.1 (13.8)	1.3 (2.2)
Spleen	3.9v10^7	1.3 (2.7)	40.2 (83.9)	5.9 (12.3)	0.54 (1.1)
Thymus	1.9 × 10^5	NE	2.1 (2.3)	89.4 (97.7)	NE
PB	NE	5.4 (12.4)	28.9 (66.3)	9.3 (21.3)	NE
Mouse no. 7/donor no. 5					
BM	1.4 × 10^7	7.2 (14.2)	39.6 (78.1)	3.1 (6.1)	0.82 (1.6)
Spleen	2.2 × 10^7	2.4 (5.1)	37.2 (79.3)	6.8 (14.5)	0.52 (1.1)
Thymus	1.3 × 10^5	NE	0.6 (0.7)	85.1 (99.2)	NE
PB	NE	2.3 (41.7)	49.3 (89.5)	3.5 (6.4)	NE
Mouse no. 8/donor no. 6					
BM	1.1 × 10^7	6.1 (11.7)	36.8 (70.6)	7.7 (14.8)	2.5 (4.8)
Spleen	2.9 × 10^7	2.9 (4.6)	33.8 (53.1)	24.6 (38.6)	2.4 (3.8)
Thymus	1.9 × 10^5	NE	1.1 (1.2)	94.1 (97.0)	NE
PB	NE	8.1 (11.9)	50.2 (73.5)	10.0 (14.6)	NE

BM, spleen, and thymus were harvested from engrafted NOD/SCID/IL2rγ^{null} mice at 3 months after transplantation. Total cell numbers in BM and thymus represent the cells harvested from 2 femurs for BM and those harvested from a hemilobe for thymus. Recipients 1, 2, 4, and 5 received transplants of 1 × 10^5 Lin$^-$CD34$^+$ cells. Recipients 6, 7, and 8 received transplants of 2 × 10^4 Lin$^-$CD34$^+$CD38$^-$ cells. NE indicates not examined.

of circulating human blood cells even 24 weeks after transplantation (not shown), suggesting the long-term engraftment of self-renewing human HSCs.

In all mice injected with Lin$^-$hCD34$^+$hCD38$^-$ cells, hGPA$^+$ erythroid cells and hCD41a$^+$ megakaryocytes were present (not shown). We then tested whether differentiation of Lin$^-$hCD34$^+$hCD38$^-$ HSCs in the NOD/SCID/IL2rγ^{null} mouse microenvironment can recapitulate normal developmental processes in the human bone marrow. We and others have reported that phenotypically separable myeloid and lymphoid progenitors are present in the steady-state normal bone marrow in both mice[38,39] and humans.[28,29] Figure 2C shows the representative FACS analysis data of recipient's bone marrow cells. In all 3 mice tested, the bone marrow contained the hCD34$^+$hCD38$^-$ HSC[36,37] and the hCD34$^+$hCD38$^+$ progenitor fractions.[28] The hCD34$^+$hCD38$^+$hCD10$^+$hCD127 (IL-7Rα)$^+$ common lymphoid progenitor (CLP) population[29] was detected (Figure 2C, top panels). According to the phenotypic definition of human myeloid progenitors,[28] the hCD34$^+$hCD38$^+$ progenitor fraction was subfractionated into hCD45RA$^-$hCD123 (IL-3Rα)^{lo} common myeloid progenitor (CMP), hCD45RA$^-$hCD123$^-$ megakaryocyte/erythrocyte progenitor (MEP), and hCD45RA$^+$hCD123^{lo} granulocyte/monocyte progenitor (GMP) populations (Figure 2C, bottom panels). We then purified these myeloid progenitors, and tested their differentiation potential. As shown in Figure 2D, purified GMPs and MEPs generated granulocyte/monocyte (GM)– and megakaryocyte/erythrocyte (MegE)–related colonies, respectively, while CMPs as well as HSCs generated mixed colonies in addition to GM and MegE colonies. These data strongly suggest that hCD34$^+$hCD38$^-$ human HSCs differentiate into all myeloid and lymphoid lineages tracking normal developmental steps of the steady-state human hematopoiesis within the NOD/SCID/IL2rγ^{null} mouse bone marrow.

Development of human systemic and mucosal immune systems in NOD/SCID/IL2rγ^{null} mice

We further evaluated development of the human immune system in NOD/SCID/IL2rγ^{null} recipients. In the thymus, thymocytes were mostly consisted of hCD3$^+$ T cells with scattered hCD19$^+$ B cells (Figure 3A-B). This is reasonable since the normal murine thymus contain a small number of B cells in addition to T cells.[40]

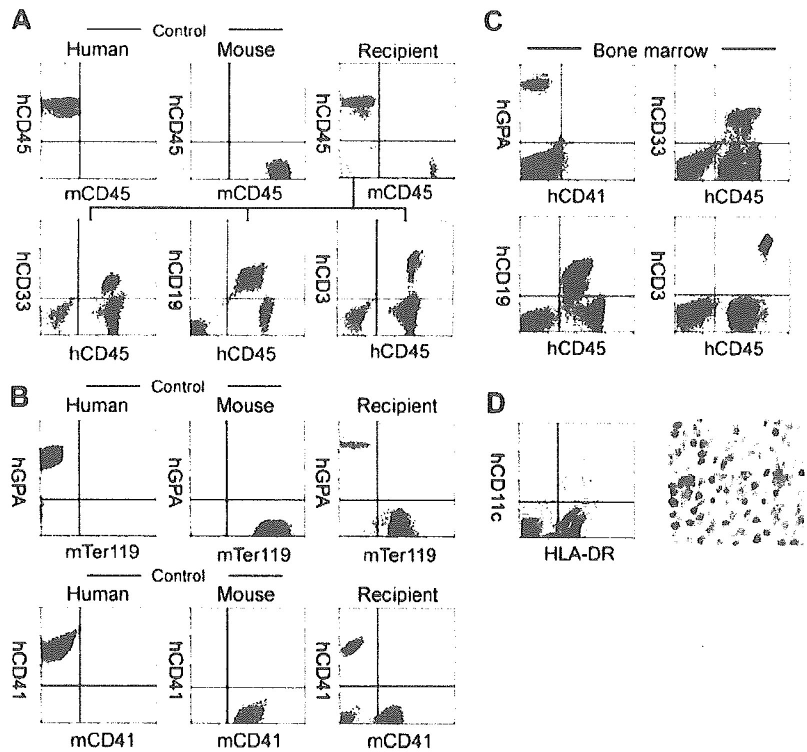

Figure 1. Analysis of human hematopoietic cells in NOD/SCID/IL2rγ^{null} recipients. (A) In the scatter gates for nucleated cells, anti-hCD45 and anti-mCD45 antibodies (Abs) reacted exclusively with human and murine leukocytes, respectively. In the recipient blood, the majority of nucleated cells were human leukocytes (top row). High levels of engraftment by hCD33$^+$ myelomonocytic cells, hCD19$^+$ B cells, and hCD3$^+$ T cells were achieved in peripheral blood of recipient mice given transplants of Lin$^-$hCD34$^+$ CB cells (bottom row). (B) Analysis of circulating erythrocytes (top row) or platelets (bottom row) in a NOD/SCID/IL2rγ^{null} recipient. In the blood, Ter119$^+$ murine erythrocytes as well as hGPA$^+$ human erythrocytes were detected. mCD41a$^+$ murine platelets were also reconstituted. (C) Multilineage engraftment of human cells in the NOD/SCID/IL2rγ^{null} murine bone marrow. hCD33$^+$ myelomonocytic cells, hCD19$^+$ B cells, and hCD3$^+$ T cells were present. hGPA$^+$ erythroid cells and hCD41a$^+$ megakaryocytes were also seen in the nucleated cell gate of the bone marrow. (D, left) HLA-DR$^+$hCD11c$^+$ dendritic cells were detected in the spleen by a flow cytometric analysis. (Right) Immunohistochemical staining of CD11c in the spleen. CD11c$^+$ cells displayed dendritic cell morphology.

Thymocytes consisted of immature hCD4$^+$hCD8$^+$ double-positive (DP) T cells (Figure 3C) as well as small numbers of hCD4$^+$ or hCD8$^+$ single-positive (SP) mature T cells (Figure 4A, top panel), while hCD3$^+$ human T cells in spleen were mainly constituted of either hCD4$^+$ or hCD8$^+$ single positive T cells (Figure 4A, bottom panel). These data suggest that normal selection processes of T-cell development may occur in the recipients' thymi.

In the spleen, lymphoid follicle-like structures were seen (Figure 3D-E), where predominant hCD19$^+$ B cells were associated with surrounding scattered hCD3$^+$ T cells (Figure 3F). Development of mesenteric lymph nodes was also observed, where the similar follicle-like structures consisted of human B and T cells were present (not shown). In the bone marrow and the spleen, nucleated cells in each organ contained hCD34$^+$hCD19$^+$ pro-B cells, hCD10$^+$hCD19$^+$ immature B cells, and hCD19$^+$hCD20$^+$ mature B cells (Figure 4B). Figure 4C shows the expression of human immunoglobulins on hCD19$^+$ B cells. A significant fraction of hCD19$^+$ B cells expressed human IgM on their surface. A

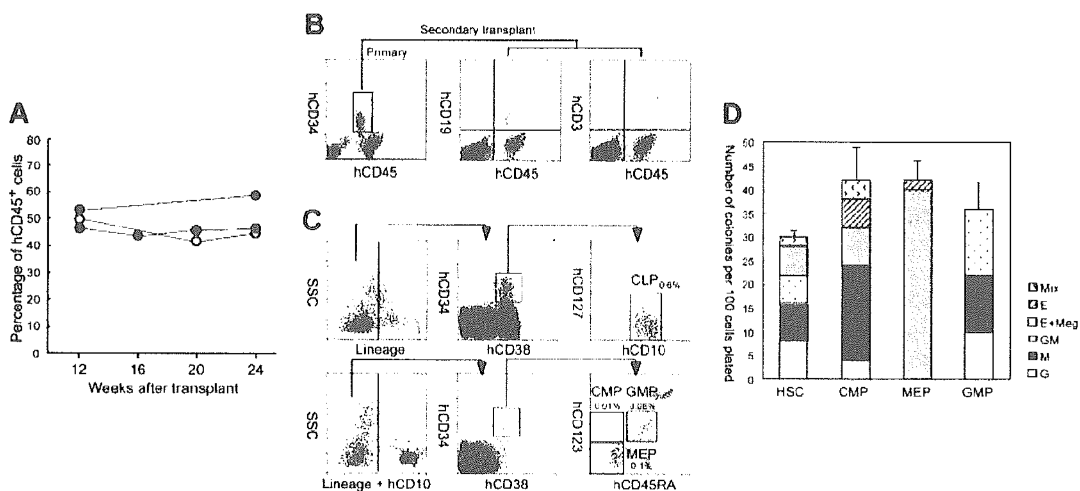

Figure 2. Purified Lin$^-$hCD34$^+$hCD38$^-$ CB cells reconstitute hematopoiesis via physiological intermediates, and display long-term reconstitution in the NOD/SCID/IL2rγ^{null} newborn system. (A) Serial evaluation of chimerism of human cells in peripheral blood of recipient mice injected with 2×10^4 Lin$^-$hCD34$^+$hCD38$^-$ CB cells. White, gray, and black dots represent 3 individual recipients. (B) hCD34$^+$ cells purified from a primary recipient marrow (left) were successfully engrafted into the secondary newborn recipients. hCD19$^+$ B cells (middle) and hCD3$^+$ T cells (right) in a representative secondary recipient is shown. (C) The Lin$^-$ bone marrow cells contained hCD34$^+$hCD38$^+$hCD10$^+$hCD127 (IL-7Rα)$^+$ CLPs (top row). In the Lin$^-$hCD10$^-$fraction, hCD34$^+$hCD38$^+$hCD45RA$^-$hCD123 (IL-3Rα)^{lo} CMPs, hCD34$^+$hCD38$^+$hCD45RA$^+$hCD123^{lo} GMPs, hCD34$^+$hCD38$^+$hCD45RA$^-$hCD123$^-$ MEPs were present. Each number for progenitors indicates percentages of hCD45$^+$ cells. SSC indicates side scatter. (D) Colony-forming activity of purified myeloid progenitor population in the methylcellulose assay. Representative data from 1 of 3 recipients are shown. Error bars represent standard deviation.

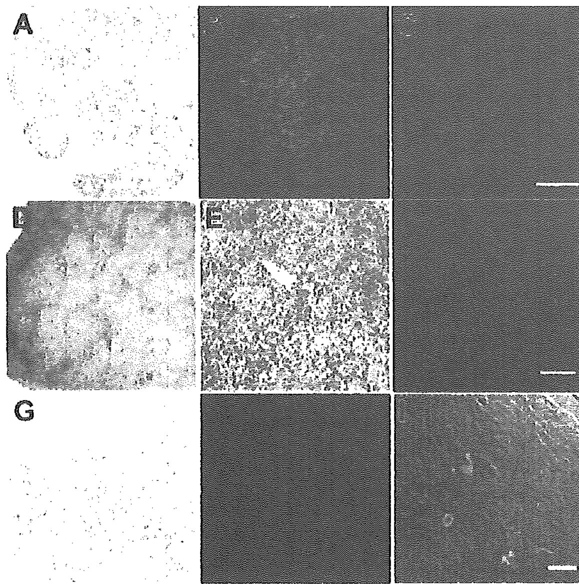

Figure 3. Histology of lymphoid organs in engrafted NOD/SCID/IL2rγ^{null} recipients. (A) The thymus showed an increased cellularity after reconstitution. (B) The thymus stained with anti-hCD3 (green) and anti-hCD19 (red) antibodies. (C) The thymus stained with anti-hCD4 (green) and anti-hCD8 (red) antibodies. The majority of thymocytes are doubly positive for hCD4 and hCD8. (D-E) Lymphoid follicle-like structures in the spleen of a recipient. (F) The lymphoid follicles mainly contained hCD19$^+$ B cells (red) that were surrounded by scattered hCD3$^+$ T cells (green). (G) Histology of the intestine in an engrafted NOD/SCID/IL2rγ^{null} recipient (left). (H) In the intestine, DAPI$^+$ (4',6-diamidino-2-phenylindole)–nucleated cells (blue) contained both scattered hCD3$^+$ T cells (green) and human IgA$^+$ cells (red). (I) The DIC image of the same section shows that IgA$^+$ B cells were mainly found in the interstitial region of the intestinal mucosal layer. White bars inside panels represent 80 μm (C), 100μm (F), and 20μm (I).

fraction of cells expressing IgD were also observed in the blood and the spleen, suggesting that class switching occurred in these developing B cells. As reported in the Rag2$^{-/-}$ γc$^{-/-}$ mouse models,[10,12,14] hCD19$^+$IgA$^+$ B cells were detected in the bone marrow and the spleen in NOD/SCID/IL2rγ^{null} recipients. We then evaluated concentrations of human immunoglobulins in sera of mice given transplants of human Lin$^-$hCD34$^+$ CB cells by ELISA. In all sera from 3 NOD/SCID/IL2rγ^{null} recipients, a significant amount of IgG (257 ± 76 μg/mL) and IgM (600 ± 197 μg/mL) were detectable, whereas sera from the control NOD/SCID/β2m$^{-/-}$ mice contained lower levels of IgM (76 ± 41 μg/mL) and little or no IgG (Table S1, available on the *Blood* website; see the Supplemental Table link at the top of the online article). These data collectively suggest that class-switching can effectively occur in NOD/SCID/IL2rγ^{null} mice.

The intestinal tract is one of the major sites for supporting host defense against exogenous antigens. Since bone marrow and spleen hCD19$^+$ B cells contained a significant fraction of cells expressing IgA, we tested whether reconstitution of mucosal immunity could be achieved in the NOD/SCID/IL2rγ^{null} recipients. Immunohistologic analyses demonstrated that the intestinal tract of recipient mice contained significant numbers of cells expressing human IgA in addition to hCD3$^+$ T cells (Figure 3G-I). Thus, human CB cells could reconstitute cells responsible for both systemic and mucosal immunity in the NOD/SCID/IL2rγ^{null} newborn system.

Function of adaptive human immunity in engrafted NOD/SCID/IL2rγ^{null} mice

Five NOD/SCID/IL2rγ^{null} mice reconstituted with 3 independent human CB samples were immunized twice with ovalbumin (OVA) at 3 months after transplantation. Two weeks after immunization, sera were collected from these immunized mice, and were subjected to ELISA to quantify OVA-specific human IgG and IgM. As shown in Figure 5A, significant levels of OVA-specific human IgM and IgG were detected in all serum samples from immunized mice, but not in samples from nonimmunized engrafted mice. Thus, the adaptive human immune system properly functioned in the NOD/SCID/IL2rγ^{null} strain to produce antigen-specific human IgM and IgG antibodies.

We next tested the alloantigen-specific cytotoxic function of human T cells developed in NOD/SCID/IL2rγ^{null} recipients. hCD3$^+$ T cells isolated from the spleen of NOD/SCID/IL2rγ^{null} recipients were cultured with allogeneic B-LCL (TAK-LCL). We established 8 hCD4$^+$ and 10 hCD8$^+$ T-cell clones responding LCL-specific allogeneic antigens. We then estimated cytotoxic activity of these T-cell clones in the presence or absence of anti–HLA-DR and anti–HLA class I antibodies. We randomly chose 3 each of CD4 and CD8 clones for further analysis (Figure 5B). A ^{51}Cr release assay revealed that both hCD4$^+$ and hCD8$^+$ T cell clones exhibited cytotoxic activity against allogeneic TAK-LCL, whereas they showed no cytotoxicity against KIN-LCL, a cell line not sharing HLA classes I or II with TAK-LCL. Cytotoxic activity of hCD4$^+$

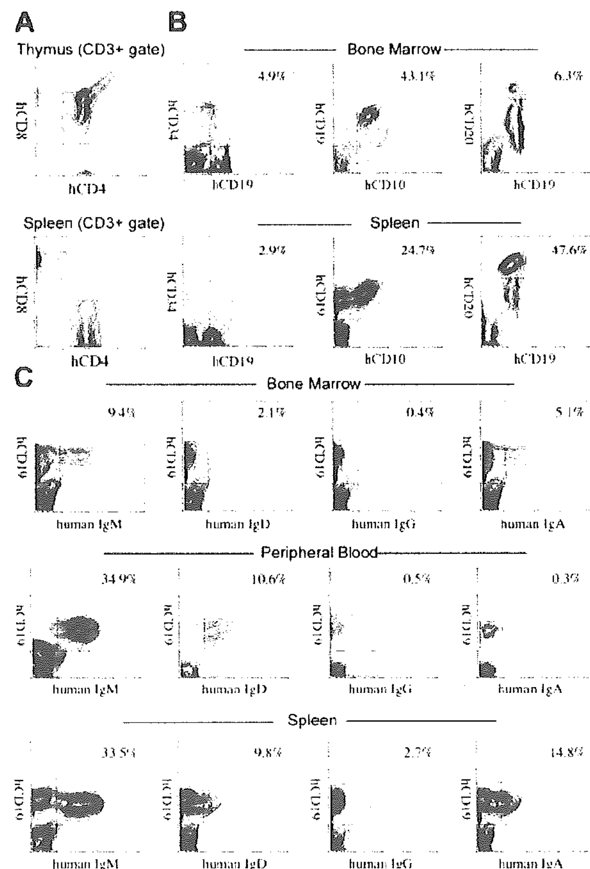

Figure 4. Development of lymphocytes in NOD/SCID/IL2rγ^{null} recipients. (A) The flow cytometric analysis of human T cells in recipients. The majority of cells in the thymus were hCD4$^+$hCD8$^+$ double-positive thymocytes (top). The CD3$^+$ spleen cells contained hCD4$^+$ or hCD8$^+$ single-positive mature T cells (bottom). (B) hCD34$^+$hCD19$^+$ pro-B, hCD10$^+$hCD19$^+$ pre-B, and hCD19$^+$hCD20^{hi} mature B cells were seen in different proportions in the bone marrow and the spleen of recipient mice. Numbers represent percentages within total nucleated cells. (C) B cells expressing each class of human immunoglobulin heavy chain were seen in the bone marrow, the peripheral blood (PB), or the spleen of engrafted NOD/SCID/IL2rγ^{null} mice. Numbers represent percentages out of nucleated cells.

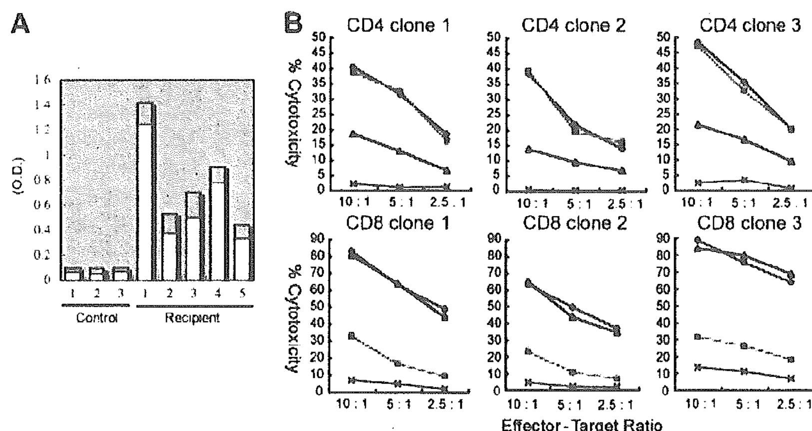

Figure 5. Functional analysis of human T and B cells developed in NOD/SCID/IL2rγ^{null} recipients. (A) Production of OVA-specific human immunoglobins. Two weeks after immunization with OVA, sera of 5 independent recipients were sampled, and were evaluated for the concentration of OVA-specific human IgM (□) and IgG (□) by ELISA. Sera of 3 nonimmunized NOD/SCID/IL2rγ^{null} recipients were used as controls. O.D. indicates optical density. (B) Cytotoxic activity of human T cells generated in NOD/SCID/IL2rg-null mice. hCD4$^+$ and hCD8$^+$ T-cell clones derived from the recipient spleen were cocultured with allogeneic target cells (TAK-LCLs). KIN-LCLs that do not share any HLA type with effector cells or TAK-LCLs (X) were used as negative controls. Both hCD4$^+$ and hCD8$^+$ T-cell lines displayed cytotoxic activity against TAK-LCL in a dose-dependent manner. In hCD4$^+$ T-cell clones, this effect was blocked by anti–HLA-DR antibodies (▲), whereas in hCD8$^+$ T-cell clones, the effect was blocked by anti–HLA class I antibodies (■). ◆ indicates cytotoxic response to TAK-LCLs without addition of antibodies.

and hCD8$^+$ T cell clones was significantly inhibited by the addition of anti–HLA-DR and anti–HLA class I antibodies, respectively. These data clearly demonstrate that human CB-derived T cells can exhibit cytotoxic activity in an HLA-restricted manner.

Discussion

Xenogeneic transplantation models have been extensively used to study human hematopoiesis in vivo.[1,41,42] In the present study, we describe a new xenogeneic transplantation system that effectively supports human hemato-lymphoid development of all lineages for the long term.

NOD/SCID/IL2rγ^{null} newborns exhibited very efficient reconstitution of human hematopoietic and immune systems after intravenous injection of a relatively small number of CB cells. In our hands, NOD/SCID/IL2rγ^{null} newborns displayed a significantly higher chimerism of human blood cells compared with NOD/SCID/β2m$^{-/-}$ newborns under an identical transplantation setting (Table 1). This result directly shows that the IL2rγ^{null} mutation has a merit on human cell engraftment over the β2m$^{-/-}$ mutation.

One of the critical problems in the NOD/SCID strain for the use of recipients is that this mouse line possesses a predisposition to thymic lymphoma due to an endogenous ectropic provirus (Emv-30).[32] Because of this, NOD/SCID and NOD/SCID/β2m$^{-/-}$ mice have the short mean lifespan of 8.5 and 6 months, respectively, while NOD/SCID/IL2rγ^{null} mice did not develop thymic lymphoma surviving more than 15 months,[31] which allows a long-term experimentation.

In our study, NOD/SCID/IL2rγ^{null} newborns injected with 10^5 hCD34$^+$ CB cells via a facial vein consistently displayed high levels of chimerism of human hematopoiesis (50%-80%; Table 1). This model is comparable to, or may be more efficient than the Rag2$^{-/-}$ γc$^{-/-}$ newborn model where intrahepatic injection of 0.4 to 1.2×10^5 hCD34$^+$ CB cells generated variable levels of chimerism of human cells (5%-65%).[14] This slight difference of engraftment efficiency, however, could reflect the homing efficiency of HSCs by each injection route. The NOD/SCID/IL2rγ^{null} newborn model might be more efficient than the NOD/SCID/$\gamma_c^{-/-}$ adult model in which the majority of recipients showed approximately 30% chimerism of human cells after transplantation of 5×10^4 hCD34$^+$ CB cells.[11] Although we did not test NOD/SCID/$\gamma_c^{-/-}$ newborns side by side in this study, we have found that the engraftment level of hCD34$^+$ cells of human acute myelogenous leukemia is approximately 3-fold higher in newborns than adults in the NOD/SCID/IL2rγ^{null} strain (F.I., T.M., S.Y., M.Y., M.H., K.A., and L.D.S., manuscript in preparation). Therefore, it remains unclear whether the IL2rγ^{null} mutation has a significant advantage over the truncated γc mutation[11] for human cell engraftment. It is still possible that the improved engraftment efficiencies in the NOD/SCID/IL2rγ^{null} newborn system as compared to those in the NOD/SCID/$\gamma_c^{-/-}$ adult system reflect the age-dependent maturation of the xenogeneic barrier.

The Rag2$^{-/-}$ γc$^{-/-}$ newborn and NOD/SCID/$\gamma_c^{-/-}$ adult models have provided definitive evidences that functional T cells, B cells, and dendritic cells can develop from hematopoietic progenitor cells in immunodeficient mice. Class-switching of immunoglobulin in CB-derived B cells properly occurred in the NOD/SCID/IL2rγ^{null} but not in the NOD/SCID/β2m$^{-/-}$ newborns (Table S1), further confirming the advantage of the NOD/SCID/IL2rγ^{null} model. We also showed that, consistent with a previous report using the Rag2$^{-/-}$ γc$^{-/-}$ model,[14] human T and B cells developed in NOD/SCID/IL2rγ^{null} mice are capable of mounting antigen-specific immune responses. Interestingly, human T and B cells migrated into murine lymphoid organs and into the intestinal tissues to collaborate in forming lymphoid organ structures. Furthermore, we found that IgA-secreting human B cells can develop in the murine intestine, suggesting that human mucosal immunity could be generated. Thus, the cellular interaction and the lymphocyte homing could occur at least to some extent across the xenogenic barrier in this model. It is also of interest that developing human cells in the thymus displayed normal distribution of SP and DP cells (Figure 4A), and that mature human T cells displayed cytotoxic functions in an HLA-dependent manner (Figure 5B). This suggests that positive and/or negative selection of human T cells could occur in NOD/SCID/IL2rγ^{null} recipients. Thymic epithelial cells in recipients reacted with anti-murine but not anti-human centromere probes in a FISH assay (F.I. and M.H., unpublished data, September 2004), confirming their recipient's origin. Thus, it remains unclear how these human T cells effectively educated and developed in murine thymus. It is also possible that human mature T cells developed by extrathymic education and selection.

Our data directly show that the most primitive hCD34$^+$hCD38$^-$ CB cells are capable of generating the human myeloerythroid system in addition to the immune system in the NOD/SCID/IL2rγ^{null} recipients. The emergence of circulating hCD33$^+$ myelomonocytic cells after transplantation of human CB cells has been reported in the NOD/SCID/β2m$^{-/-}$ newborn[33] and the NOD/SCID/$\gamma_c^{-/-}$ adult[11] systems. Development of human erythropoiesis, however, has not been obtained in previous models,

although it has been reported that NOD/SCID mice can support terminal maturation of hCD71$^+$ erythroblasts that were induced ex vivo from human HSCs by culturing with human cytokines.[43] We showed for the first time that human erythropoiesis and thrombopoiesis can develop in mice from primitive hCD34$^+$hCD38$^-$ cells, as evidenced by the presence of erythroblasts and megakaryocytes in the bone marrow and of circulating erythrocytes and platelets in NOD/SCID/IL2rγ^{null} recipients. It is important to note that the hCD34$^+$hCD38$^-$ CB HSC population generated myeloid- and lymphoid-restricted progenitor populations such as CMPs, GMPs, MEPs, and CLPs in the bone marrow (Figure 2E-F). Thus, the NOD/SCID/IL2rγ^{null} microenvironment might be able to support physiological steps of myelopoiesis and lymphopoiesis initiating from the primitive HSC stage.

In summary, we show that the NOD/SCID/IL2rγ^{null} newborn system efficiently supports hemato-lymphoid development from primitive human HSCs, passing through physiological developmental intermediates. It also can support development of human systemic and mucosal immunity, and therefore may be useful to use human immunity to produce immunoglobulins or experimental vaccines. The NOD/SCID/IL2rγ^{null} newborn system might also serve as an efficient tool for understanding malignant hematopoiesis in humans, since the analysis of human leukemogenesis has mainly been dependent upon the NOD/SCID adult mouse system.[44-46] Our model might also be useful to reproduce the transforming process of human hematopoietic cells, as transplanted murine hematopoietic progenitor and stem cells can develop leukemia by transducing oncogenic fusion genes in syngeneic mouse models.[47,48] Thus, the use of this system should open a more efficient way to analyze normal and malignant human hematopoiesis.

Acknowledgments

We thank Bruce Gott and Lisa Burzenski for excellent technical assistance, and Dr Sato and other staff at Fukuoka Cord Blood Bank for preparation of CB.

References

1. Greiner DL, Hesselton RA, Shultz LD. SCID mouse models of human stem cell engraftment. Stem Cells. 1998;16:166-177.
2. McCune JM, Namikawa R, Kaneshima H, Shultz LD, Lieberman M, Weissman IL. The SCID-hu mouse: murine model for the analysis of human hematolymphoid differentiation and function. Science. 1988;241:1632-1639.
3. Mosier DE, Gulizia RJ, Baird SM, Wilson DB. Transfer of a functional human immune system to mice with severe combined immunodeficiency. Nature. 1988;335:256-259.
4. Kaneshima H, Namikawa R, McCune JM. Human hematolymphoid cells in SCID mice. Curr Opin Immunol. 1994;6:327-333.
5. Pflumio F, Izac B, Katz A, Shultz LD, Vainchenker W, Coulombel L. Phenotype and function of human hematopoietic cells engrafting immune-deficient CB17-severe combined immunodeficiency mice and nonobese diabetic-severe combined immunodeficiency mice after transplantation of human cord blood mononuclear cells. Blood. 1996;88:3731-3740.
6. Shultz LD, Lang PA, Christianson SW, et al. NOD/LtSz-Rag1null mice: an immunodeficient and radioresistant model for engraftment of human hematolymphoid cells, HIV infection, and adoptive transfer of NOD mouse diabetogenic T cells. J Immunol. 2000;164:2496-2507.
7. Goldman JP, Blundell MP, Lopes L, Kinnon C, Di Santo JP, Thrasher AJ. Enhanced human cell engraftment in mice deficient in RAG2 and the common cytokine receptor gamma chain. Br J Haematol. 1998;103:335-342.
8. Greiner DL, Shultz LD, Yates J, et al. Improved engraftment of human spleen cells in NOD/LtSz-scid/scid mice as compared with C.B-17-scid/scid mice. Am J Pathol. 1995;146:888-902.
9. Yoshino H, Ueda T, Kawahata M, et al. Natural killer cell depletion by anti-asialo GM1 antiserum treatment enhances human hematopoietic stem cell engraftment in NOD/Shi-scid mice. Bone Marrow Transplant. 2000;26:1211-1216.
10. Kollet O, Peled A, Byk T, et al. beta2 microglobulin-deficient (B2m(null)) NOD/SCID mice are excellent recipients for studying human stem cell function. Blood. 2000;95:3102-3105.
11. Ito M, Hiramatsu H, Kobayashi K, et al. NOD/SCID/gamma(c)(null) mouse: an excellent recipient mouse model for engraftment of human cells. Blood. 2002;100:3175-3182.
12. Hiramatsu H, Nishikomori R, Heike T, et al. Complete reconstitution of human lymphocytes from cord blood CD34+ cells using the NOD/SCID/gammacnull mice model. Blood. 2003;102:873-880.
13. Leonard WJ. Cytokines and immunodeficiency diseases. Nat Rev Immunol. 2001;1:200-208.
14. Traggiai E, Chicha L, Mazzucchelli L, et al. Development of a human adaptive immune system in cord blood cell-transplanted mice. Science. 2004;304:104-107.
15. Ohbo K, Suda T, Hashiyama M, et al. Modulation of hematopoiesis in mice with a truncated mutant of the interleukin-2 receptor gamma chain. Blood. 1996;87:956-967.
16. Cao X, Shores EW, Hu-Li J, et al. Defective lymphoid development in mice lacking expression of the common cytokine receptor gamma chain. Immunity. 1995;2:223-238.
17. DiSanto JP, Muller W, Guy-Grand D, Fischer A, Rajewsky K. Lymphoid development in mice with a targeted deletion of the interleukin 2 receptor gamma chain. Proc Natl Acad Sci U S A. 1995;92:377-381.
18. Asao H, Takeshita T, Ishii N, Kumaki S, Nakamura M, Sugamura K. Reconstitution of functional interleukin 2 receptor complexes on fibroblastoid cells: involvement of the cytoplasmic domain of the gamma chain in two distinct signaling pathways. Proc Natl Acad Sci U S A. 1993;90:4127-4131.
19. Takeshita T, Asao H, Ohtani K, et al. Cloning of the gamma chain of the human IL-2 receptor. Science. 1992;257:379-382.
20. Russell SM, Keegan AD, Harada N, et al. Interleukin-2 receptor gamma chain: a functional component of the interleukin-4 receptor. Science. 1993;262:1880-1883.
21. Noguchi M, Nakamura Y, Russell SM, et al. Interleukin-2 receptor gamma chain: a functional component of the interleukin-7 receptor. Science. 1993;262:1877-1880.
22. Kondo M, Takeshita T, Higuchi M, et al. Functional participation of the IL-2 receptor gamma chain in IL-7 receptor complexes. Science. 1994;263:1453-1454.
23. Kondo M, Takeshita T, Ishii N, et al. Sharing of the interleukin-2 (IL-2) receptor gamma chain between receptors for IL-2 and IL-4. Science. 1993;262:1874-1877.
24. Ferrag F, Pezet A, Chiarenza A, et al. Homodimerization of IL-2 receptor beta chain is necessary and sufficient to activate Jak2 and downstream signaling pathways. FEBS Lett. 1998;421:32-36.
25. Reichel M, Nelson BH, Greenberg PD, Rothman PB. The IL-4 receptor alpha-chain cytoplasmic domain is sufficient for activation of JAK-1 and STAT6 and the induction of IL-4-specific gene expression. J Immunol. 1997;158:5860-5867.
26. Shultz LD, Lyons BL, Burzenski LM, et al. Human lymphoid and myeloid cell development in NOD/LtSz-scid IL2rgnull mice engrafted with mobilized human hematopoietic stem cells. J Immunol. 2005;174:6477-6489.
27. Sands MS, Barker JE, Vogler C, et al. Treatment of murine mucopolysaccharidosis type VII by syngeneic bone marrow transplantation in neonates. Lab Invest. 1993;68:676-686.
28. Manz MG, Miyamoto T, Akashi K, Weissman IL. Prospective isolation of human clonogenic common myeloid progenitors. Proc Natl Acad Sci U S A. 2002;99:11872-11877.
29. Galy A, Travis M, Cen D, Chen B. Human T, B, natural killer, and dendritic cells arise from a common bone marrow progenitor cell subset. Immunity. 1995;3:459-473.
30. LeBien TW. Fates of human B-cell precursors. Blood. 2000;96:9-23.
31. Yanai F, Ishii E, Kojima K, et al. Essential roles of perforin in antigen-specific cytotoxicity mediated by human CD4+ T lymphocytes: analysis using the combination of hereditary perforin-deficient effector cells and Fas-deficient target cells. J Immunol. 2003;170:2205-2213.
32. Prochazka M, Gaskins HR, Shultz LD, Leiter EH. The nonobese diabetic scid mouse: model for spontaneous thymomagenesis associated with immunodeficiency. Proc Natl Acad Sci U S A. 1992;89:3290-3294.
33. Ishikawa F, Livingston AG, Wingard JR, Nishikawa S, Ogawa M. An assay for long-term engrafting human hematopoietic cells based on newborn NOD/SCID/beta2-microglobulin(null) mice. Exp Hematol. 2002;30:488-494.
34. Kina T, Ikuta K, Takayama E, et al. The monoclonal antibody TER-119 recognizes a molecule associated with glycophorin A and specifically marks the late stages of murine erythroid lineage. Br J Haematol. 2000;109:280-287.
35. Okuno Y, Iwasaki H, Huettner CS, et al. Differential regulation of the human and murine CD34 genes in hematopoietic stem cells. Proc Natl Acad Sci U S A. 2002;99:6246-6251.
36. Craig W, Kay R, Cutler RL, Lansdorp PM. Expression of Thy-1 on human hematopoietic progenitor cells. J Exp Med. Vol. 177; 1993:1331-1342.
37. Terstappen LW, Huang S, Safford M, Lansdorp